

**Center for Electronics and  
Electrical Engineering**

# **Technical Progress Bulletin**

Covering Center Programs,  
October to December 1989,  
with 1990 CEEE Events Calendar

**U.S. DEPARTMENT OF COMMERCE  
National Institute of Standards  
and Technology  
Center for Electronics and  
Electrical Engineering  
Semiconductor Electronics Division  
Gaithersburg, MD 20899**

**June 1990**

# **89-4**

**U.S. DEPARTMENT OF COMMERCE  
Robert A. Mosbacher, Secretary  
NATIONAL INSTITUTE OF STANDARDS  
AND TECHNOLOGY  
Dr. John W. Lyons, Director**

**NIST**



**Center for Electronics and  
Electrical Engineering**

# **Technical Progress Bulletin**

Covering Center Programs,  
October to December 1989,  
with 1990 CEEE Events Calendar

**U.S. DEPARTMENT OF COMMERCE  
National Institute of Standards  
and Technology  
Center for Electronics and  
Electrical Engineering  
Semiconductor Electronics Division  
Gaithersburg, MD 20899**

**June 1990**

# **89-4**



**U.S. DEPARTMENT OF COMMERCE  
Robert A. Mosbacher, Secretary  
NATIONAL INSTITUTE OF STANDARDS  
AND TECHNOLOGY  
Dr. John W. Lyons, Director**

## INTRODUCTION TO JUNE 1990 ISSUE OF THE CEEE TECHNICAL PROGRESS BULLETIN

This is the twenty-ninth issue of a quarterly publication providing information on the technical work of the National Institute of Standards and Technology (formerly the National Bureau of Standards) Center for Electronics and Electrical Engineering. This issue of the CEEE Technical Progress Bulletin covers the fourth quarter of calendar year 1989.

Organization of Bulletin: This issue contains abstracts for all Center papers released for publication by NIST in the quarter and citations and abstracts for Center papers published in the quarter. Entries are arranged by technical topic as identified in the table of contents and alphabetically by first author under each subheading within each topic. Unpublished papers appear under the subheading "Released for Publication." Papers published in the quarter appear under the subheading "Recently Published." Following each abstract is the name and telephone number of the individual to contact for more information on the topic (usually the first author). This issue also includes a calendar of Center conferences and workshops planned for calendar year 1990 and a list of sponsors of the work.

Center for Electronics and Electrical Engineering: Center programs provide national reference standards, measurement methods, supporting theory and data, and traceability to national standards.

The metrological products of these programs aid economic growth by promoting equity and efficiency in the marketplace, by removing metrological barriers to improved productivity and innovation, by increasing U. S. competitiveness in international markets through facilitation of compliance with international agreements, and by providing technical bases for the development of voluntary standards for domestic and international trade. These metrological products also aid in the development of rational regulatory policy and promote efficient functioning of technical programs of the Government.

The work of the Center is divided into two major programs: the Semiconductor Technology Program, carried out by the Semiconductor Electronics Division in Gaithersburg, MD, and the Signals and Systems Metrology Program, carried out by the Electricity Division in Gaithersburg and the Electromagnetic Fields and Electromagnetic Technology Divisions in Boulder, CO. Key contacts in the Center are given on the back cover; readers are encouraged to contact any of these individuals for further information. To request a subscription or for more information on the Bulletin, write to CEEE Technical Progress Bulletin, National Institute of Standards and Technology, Metrology Building, Room B-358, Gaithersburg, MD 20899 or call (301) 975-2220.

Center sponsors: The Center Programs are sponsored by the National Institute of Standards and Technology and a number of other organizations, in both the Federal and private sectors; these are identified on page 42.

Note on Publication Lists: Guides to earlier as well as recent work are the publication lists covering the work of each division. These lists are revised and reissued on an approximately annual basis and are available from the originating division. The current set is identified in the Additional Information section, page 35.

TABLE OF CONTENTS

INTRODUCTION . . . . . inside title page

SEMICONDUCTOR TECHNOLOGY PROGRAM . . . . . 2

    Silicon Materials . . . . . 2

    Dimensional Metrology . . . . . 2

    Analysis Techniques . . . . . 2

    Photodetectors . . . . . 3

    Device Physics and Modeling . . . . . 4

    Insulators and Interfaces . . . . . 5

    Packaging . . . . . 6

    Other Semiconductor Metrology Topics . . . . . 7

SIGNALS & SYSTEMS METROLOGY PROGRAM . . . . . 8

FAST SIGNAL ACQUISITION, PROCESSING, & TRANSMISSION . . . . . 8

    Waveform Metrology . . . . . 8

    DC & Low Frequency Metrology . . . . . 8

    Fundamental Electrical Measurements . . . . . 9

    Cyroelectronic Metrology . . . . . 9

    Antenna Metrology . . . . . 11

    Microwave & Millimeter-Wave Metrology . . . . . 14

    Optical Fiber Metrology . . . . . 16

    Electro-Optic Metrology . . . . . 16

    Electromagnetic Properties . . . . . 19

    Complex Testing . . . . . 20

    Other Fast Signal Topics . . . . . 20

ELECTRICAL SYSTEMS . . . . . 22

    Power Systems Metrology . . . . . 22

    Superconductors . . . . . 26

    Magnetic Materials & Measurements . . . . . 32

ELECTROMAGNETIC INTERFERENCE . . . . . 32

    Radiated Electromagnetic Interference . . . . . 32

ADDITIONAL INFORMATION . . . . . 35

1990 CEEE CALENDAR . . . . . 41

SPONSOR LIST . . . . . 41

KEY CONTACTS IN CENTER, CENTER ORGANIZATION . . . . . back cover

## SEMICONDUCTOR TECHNOLOGY PROGRAM

Silicon Materials

## Recently Published

Krause, S.J., Visitserngtrakul, S., Cordts, B.F., and Roitman, P., **Effect of Annealing Conditions on Precipitate and Defect Evolution in Oxygen Implanted SOI Material**, Proceedings of the 1989 IEEE SOS/SOI Technology Conference, Stateline, Nevada, October 3-5, 1989, pp. 81-82.

Silicon wafers were implanted with oxygen to a dose of  $1.8 \times 10^{18} \text{ cm}^{-2}$  at 200 keV at a temperature of 620 °C. The wafers were annealed at temperatures between 1250 and 1350 °C for times between 1 and 6 hours in a nitrogen or argon ambient. The wafers were studied with a scanned electron microscope, a transmission electron microscope, and by secondary ion mass spectrometry. For a given annealing ambient, there is a threshold temperature for the reduction and elimination of precipitates and associated lateral dislocations in the range of 1300 °C to 1325 °C. Nitrogen ambients result in nitrogen pileup at the oxide interfaces.

[Contact: Peter Roitman, (301) 975-2077]

Dimensional Metrology

## Recently Published

Postek, M.T., **Scanning Electron Microscope-Based Metrological Electron Microscope System and New Prototype Scanning Electron Microscope Magnification Standard**, Scanning Microscopy, Vol. 3, No. 4, unpagged (1989).

A metrological electron microscope has been developed at the National Institute of Standards and Technology traceable to national standards of length, and a new prototype magnification standard meeting the current needs of the scanning electron microscope (SEM) user community has been fabricated. This metrology

instrument is designed to certify standards for the calibration of the magnification of the SEM and for the certification of artifacts for linewidth measurement done in the SEM. The artifacts will be useful for various applications in which the SEM is currently being used. The SEM-based metrology system is now operational at the Institute, and its design criteria and the progress on the characterization of the instrument are presented. The design and criteria for the new lithographically produced SEM low accelerating voltage magnification standard to be calibrated on this system are also discussed.

[Contact: Beverly Wright, (301) 975-2166]

Postek, M.T., Larrabee, R.D., and Keery, W.J., **A New Approach to Accurate X-Ray Mask Measurements in a Scanning Electron Microscope**, IEEE Transactions on Electron Devices, Vol. 36, No. 11, pp. 2452-2457 (November 1989).

This paper presents the basic concept and some preliminary experimental data on a new method for measuring critical dimensions on masks used for X-ray lithography. The method uses a scanning electron microscope in a transmitted-electron imaging mode and can achieve nanometer precision. Use of this technique in conjunction with measurement algorithms derived from electron-beam-interaction modeling may ultimately enable measurements of these masks to be made to nanometer accuracy. Furthermore, since a high-contrast image results, this technique lends itself well to automated mask defect recognition and inspection.

[Contact: Beverly Wright, (301) 975-2166]

Analysis Techniques

## Released for Publication

Kopanski, J.J., Albers, J., Carver, G.P., and Ehrstein, J.R., **Verification of the Relation Between Two-Probe and**

Analysis Techniques (cont'd.)**Four-Probe Resistances as Measured on Silicon Wafers.**

The predicted relation between the two-probe resistance (spreading resistance) and the four-probe resistance, and the dependence of the four-probe resistance on the ratio of layer thickness to probe spacing have been experimentally verified. The verified behavior is predicted from calculations, based upon the solution of Laplace's equation, of the two- and four-probe resistance for arbitrary, vertical resistivity profiles. Arrays of lithographically fabricated, geometrically well-defined contacts on silicon wafers were utilized to make the necessary precise, reproducible resistance measurements. Additional measurements using point pressure contacts were also made. For verification of the two-probe--four-probe relation, silicon that was very uniform in lateral (across the surface) resistivity was used. This ensured that the variation in spreading resistance with probe spacing was large compared to any lateral variations in resistivity. The dependence of the four-probe resistance on the ratio of layer thickness to probe spacing was verified for both the in-line and square-probe configurations. Wafers that were junction isolated or back oxidized (to approximate an insulating back boundary) and p-type wafers with a back metallization (to approximate a conducting back boundary) were used. Layer thickness-to-probe-spacing ratios were varied from 0.003 to 20. Silicon wafers with resistivities between 0.0006 and 160  $\Omega$ -cm were used.

[Contact: Joseph J. Kopanski, (301) 975-2089]

Photodetectors

Released for Publication

Geist, J., Gardner, J.L., and Wilkinson, F.J., **Surface-Field Induced Feature in**

**the Quantum Yield of Silicon near 3.5 eV.**

A broad feature near 3.5 eV was observed in the internal quantum efficiency spectra of various silicon photodiodes. This appears to be the first time this feature has been reported. The feature was clearly resolved in spectra from photodiodes with strong surface fields at the oxide-silicon interface, but was small enough to preclude observation in published spectra for photodiodes with nearly flat-band conditions at the interface. The feature is attributed to a local maximum in the quantum yield for electron-hole pair production that is expected at direct transitions in the vicinity of the  $\Gamma$  point in the silicon Brillouin Zone. Qualitative arguments suggest that the magnitude of the feature increases with increasing surface field due to field-assisted impact ionization and, in the case of depleted surfaces, also due to band-gap narrowing in the surface depletion region.

[Contact: Jon Geist, (301) 975-2066]

Kohler, R., Geist, J., and Luther, J.E., **A Reflectometer for Measurements of Scattering from Photodiodes and Other Low Scattering Surfaces.**

We have designed and tested a simple instrument to measure the diffuse reflectance of good quality optical surfaces such as the surfaces of semiconductor detectors. Measurements have been performed on silicon-photodiodes and on a sample of known reflectance at two different wavelengths.

[Contact: Jon Geist, (301) 975-2066]

Recently Published

Geist, J., **Current Status of, and Future Directions in, Silicon Photodiode Self-Calibration**, Proceedings of SPIE (The International Society for Optical Engineering, P.O. Box 20, Bellingham, Washington 98227), Optical Radiation Measurements II, Vol. 1109, pp. 246-256 (1989).

Photodetectors (cont'd.)

The current status of silicon photodiode self-calibration and its applications are reviewed, including the results of a number of intercomparisons that establish the suitability of self-calibration for high-accuracy metrology applications. Some current research directions known to the author are described, and possible future directions are considered.

[Contact: Jon Geist, (301) 975-2066]

Geist, J., Stapelbroek, M. G., and Petroff, M. D., **The Absorption Cross Section of As in Si**, Proceedings of SPIE (The International Society for Optical Engineering, P.O. Box 20, Bellingham, Washington 98227), Test and Evaluation of Infrared Detectors and Arrays, Vol. 1108, pp. 51-55 (1989).

Infrared absorption cross sections of As in Si near zero Kelvin have recently been measured in two different investigations. The average of the integrals of the cross section over photon wavenumber was  $8.64 \times 10^{-13} \text{ cm}^{-1}$ . This is nearly equal to the value predicted by the oscillator-strength sum rule. Between 500 and  $1000 \text{ cm}^{-1}$ , the absorption cross sections reported here agree very well with 0.7 times the currently accepted formula for the photoionization cross section of As in Si. Calibration errors in spreading resistance measurements on epitaxial layers seem to be the cause of the 0.7 multiplicative error in the photoionization formula. Above  $1000 \text{ cm}^{-1}$ , 0.7 times the value from the formula predicts a larger photoionization cross section than the absorption cross section reported here. This is apparently caused by the impact ionization of donor electrons from impurity atoms by energetic photoionized electrons.

[Contact: Jon Geist, (301) 975-2066]

Rasmussen, A.L., Simpson, P.A., and Sanders, A.A., **Improved Low-Level Silicon-Avalanche-Photodiode Transfer**

**Standards at 1.064 Micrometers**, NISTIR 89-3917 (August 1989).

Three silicon-avalanche-photodiode transfer standards (APD TS) were calibrated from  $\approx 10^{-8}$  to  $\sim 10^{-5} \text{ W/cm}^2$  peak power density at approximately 10% uncertainty. Calibrations were performed for  $1.064\text{-}\mu\text{m}$  wavelength pulses, having 10- to 100-ns durations. For this calibration, an acousto-optically modulated laser beam provided alternately equal levels of pulsed power and cw power into a low-level beam splitter. The cw power measured by a transfer standard in the transmitted beam of the splitter was used to determine the pulsed power into the APD transfer standard in one of the low-level reflected beams of the splitter. The APD detector had about  $1\text{-cm}^2$  aperture and a 3.8-cm focal length lens in front of it. Lens, window, and detector surfaces had narrow-band anti-reflection coatings. The commercial detector package is a temperature-compensated, infrared-enhanced APD preamplifier module. To increase the sensitivity, one or two 20-dB, 500-MHz band-width amplifiers followed the preamplifier. At very low pulsed power levels, a 30-MHz low-pass filter with gaussian roll-off was attached to the amplifier output to reduce the noise. A transient digitizer recorded the impulse responses of the APD detectors at  $1.064 \mu\text{m}$ . These data were read into computer programs that convolved the unity area impulse response with unity height gaussian pulses. From these data, correction factors of the pulse peak for observed pulse durations from 10 to 100 ns were determined. Instructions, calibrations, error budgets, and system descriptions are included.

[Contact: Alvin L. Rasmussen, (303) 497-5367]

Device Physics and Modeling

## Recently Published

Gaitan, M., Enlow, E.W., and Russell, T.J., **Accuracy of the Charge Pumping**

Device Physics and Modeling (cont'd.)

**Technique for Small Geometry MOSFETs**, IEEE Transactions on Nuclear Science, Vol. NS-36, No. 6, pp. 1990-1997 (December 1989).

The channel length dependence of the charge pumping current for MOSFETs is investigated using a two-dimensional simulation technique. The dependence of charge pumping current on signal offset voltage for various MOSFET channel lengths is studied using energy-dependent interface trap distributions. Simulations are compared to experimental charge pumping measurements on irradiated MOSFETs with different gate lengths with good agreement for the shape of the curves. It is found that as the effective channel length decreases, the accepted charge pumping model has decreasing accuracy that results in an underestimation of the mean interface trap density. The loss in accuracy is due to the nonuniformity of surface potential across the channel caused by source/drain proximity. Using the charge pumping technique to measure interface trap densities on advanced devices with an effective channel length less than 1  $\mu\text{m}$  may result in unacceptable errors.

[Contact: Michael Gaitan, (301) 975-2070]

Gaitan, M., and Roitman, P., **Small Signal Modeling of the MOSOS Capacitor**, Proceedings of the 1989 IEEE SOS/SOI Technology Conference, Stateline, Nevada, October 3-5, 1989, pp. 48-49.

The high-frequency and quasi-static capacitance of an MOS capacitor on a layer of insulator metal-oxide-silicon-oxide-silicon (MOSOS) has been modeled using numerical solution by perturbation analysis of the basic semiconductor equations.

[Contact: Michael Gaitan, (301) 975-2070]

Lowney, J.R., **The Effect of Electron-Hole Plasmas on the Density of States**

**of Silicon and GaAs**, J. Appl. Phys., Vol. 66, No. 9, pp. 4279-4283 (1 November 1989).

The densities of states of the conduction and valence bands of silicon and GaAs have been calculated at 300 K for the case of an electron-hole plasma, which can occur at high-injection levels in bipolar devices or in bulk material under intense optical excitation. The results show considerable narrowing of the band gap, which needs to be included in the analysis of device measurements or the interpretation of photoluminescence data. Furthermore, the band-gap narrowing that results from dopant ions is reduced by excess carriers because of the reduced free-carrier screening radius.

[Contact: Jeremiah R. Lowney, (301) 975-2048]

Insulators and Interfaces

Released for Publication

Chandler-Horowitz, D., Marchiando, J.F., and Belzer, B.J., **Ellipsometry SRM's for Use in Thin Film Measurements**, to be published in the Proceedings of the Measurement Science Conference (MSC), Anaheim, California, February 8-9, 1990.

A Standard Reference Material (SRM) consisting of a film of silicon dioxide on a silicon substrate has been designed, fabricated, measured, and certified at the National Institute of Standards and Technology for the ellipsometric angles,  $\Delta$  and  $\psi$ , and for the derived film thickness and refractive index. This SRM can be used as an aid in the evaluation of the performance of optical and mechanical thickness-monitoring instruments as well as ellipsometers. The optical instruments are based on the theory describing reflection of light from a sample. The film thickness is determined by using a model having one or two uniform isotropic films atop a substrate. The calculated thicknesses rely on accurate

Insulators and Interfaces (cont'd.)

values of the indices of refraction of the substrate and/or film at the necessary wavelengths. The measurement procedure used here to certify the ellipsometric angles utilizes an accurate rotating-analyzer ellipsometer and HeNe laser source operating near the principal angle of incidence. The measurement data from several samples are analyzed collectively to determine the certified film thicknesses and refractive index. At the present time, three different film thicknesses, 50, 100, and 200 nm, are being certified. Future work may involve certifying thinner layers of oxides.

[Contact: Deane Chandler-Horowitz, (301) 975-2084]

Marchiando, J.F., **Semiconductor Measurement Technology: A Software Program for Aiding the Analysis of Ellipsometric Measurements, Simple Spectroscopic Models**, to be published as NIST Special Publication 400-84.

MAIN2 is a software program for the analysis of spectroscopic ellipsometric measurements. MAIN2 consists mainly of subroutines written in FORTRAN that are used to invert the standard reflection ellipsometry equations for simple systems. Here, a system is said to be simple if the solid material sample is characterized by models which assume at least the following: (1) materials are nonmagnetic; (2) samples exhibit depth-dependent optical properties, such as one with layered or laminar structure atop a substrate that behaves like a semi-infinite half-space; (3) layers are flat and of uniform thickness; and (4) the optical medium within each ambient/layer/substrate is isotropic, homogeneous, local, and linear. The ambient region refers to that region of space which lies external to the layer/substrate structure of the sample. Usually, the ambient region involves a medium of air or vacuum. Each layer is characterized by a thickness and a dielectric function. The dielectric

function of a region, i.e., ambient, layer, or substrate, is represented by the Bruggeman effective medium approximation (EMA). Within the EMA, the effective medium of a region is characterized by an aggregate mixture of constituent media, and the dielectric function of each constituent medium is known a priori. The constituent dielectric functions are taken from the literature. The ellipsometric equations are formulated as a standard damped nonlinear least-squares problem and then solved by an iterative method when possible. The program is sufficiently modular to allow one to modify some of the models used in the calculations.

[Contact: Jay F. Marchiando, (301) 975-2088]

Packaging

Recently Published

Harman, G.G., **Reliability and Yield Problems of Wire Bonding in Microelectronics, The Application of Materials and Interface Science**, International Society for Hybrid Microelectronics (ISHM) Monograph, (1989), 202 pages.

This book describes the conditions for making reliable wire bonds with a high yield by describing all potential sources of failures, from the final stages of wafer processing, through handling, bonding, testing, and screening. Sources of contamination are identified that adversely affect the reliability of wire bonds. In addition, the degrading effects of temperature, temperature cycling, and mechanical forces such as ultrasonic cleaning are described. Bonding machine setup parameters also play a critical role. In addition, the severity of the above problems may depend on the ambient atmosphere, the metallurgy of the wire, and/or the morphology of the bonding pad metallization. Wafer sawing and die attach can also adversely affect bond quality.

Basic concepts of bonding methods, wire

Packaging (cont'd.)

metallurgy and aging, and cleaning techniques (uv and/or ozone, solvent, plasma, and burnishing) are described. Classical plague failure, its metallurgy, and the effect of corrosion and impurities are extensively treated. All bond testing methods are described and compared. Problems with electroplating, various metal systems, and machines and setup are described. Thermal and ultrasonic effects on wire fatigue are discussed. Mechanical problems as cratering, cracks in wedge bonds, and the effect of acceleration and vibration are extensively given.

[Contact: George G. Harman, (301) 975-2097]

Other Semiconductor Metrology Topics

## Recently Published

Belanger, B.C., Bennett, H.S., Linholm, L.W., Russell, T.J., and Schafft, H.A., **Technology Transfer at NIST**, Proceedings of the 1989 Government Microcircuit Applications Conference (GOMAC), Orlando, Florida, November 7-9, 1989, pp. 1-9.

The National Institute of Standards and Technology (NIST), has been engaged in semiconductor device and materials research and development for many years. NIST emphasized technology transfer to industry and other government agencies long before "tech transfer" became as fashionable as it is today. For semiconductor electronics as well as for other fields, NIST generally does not engage in product development, but rather emphasizes measurement and test methods and quality assurance tools needed throughout the microelectronics industry. We choose our priorities to complement research and development under way in industry, universities, and other government agencies.

Work in semiconductor electronic devices and materials is primarily in NIST's Center for Electronics and Electrical

Engineering (CEEE), which also includes work in electrical and electronic instrumentation and standards, electric power and energy measurements, microwaves, lightwaves, and superconducting materials and devices. Work on linewidth measurements is carried out by NIST's Center for Manufacturing Engineering (CME). This paper describes the mechanisms that CEEE and CME have found effective and concludes with several examples of technology which has been transferred or is being transferred.

[Contact: Robert I. Scace, (301) 975-2220]

Kopanski, J.J., and Novotny, D.B., **Electrical Characterization of Beta Silicon Carbide MIS Capacitors with Thermally Grown or Chemical-Vapor-Deposited Oxides**, Extended Abstract of the Electrochemical Society Meeting, Hollywood, Florida, October 15-20, 1989, pp. 722-723.

Metal-Insulator-Semiconductor (MIS) capacitors were fabricated on beta silicon carbide single crystals. The insulating layers were thermally grown oxides or chemical-vapor-deposited oxides. Various oxidation conditions and post-deposition densification treatments were investigated. Capacitors were characterized by capacitance-voltage measurements. The effects of measurement frequency, voltage sweep rate, illumination, and temperature (to 300 °C) on the C-V response were determined. Interface trap distributions were estimated from the high-frequency capacitance. Oxide fixed charges were 5 to 9 x 10<sup>11</sup> cm<sup>-2</sup>, and interface trapped charge density at mid-gap levels was 0.5 to 2.0 x 10<sup>11</sup> cm<sup>-2</sup> eV<sup>-1</sup>.

[Contact: Joseph J. Kopanski, (301) 975-2089]

Littler, C.L., Zawadzki, W., Looee, M.R., Song, X.N., and Seiler, D.G., **Donor-Shifted Phonon-Assisted Magneto-Optical Resonances in N-InSb**, Physical Review Letters, Vol. 63, No. 26, pp.

Other Semiconductor Topics (cont'd.)

2845-2848 (25 December 1989).

We have observed and described new optical transitions between magneto-donor states in InSb, both with and without optic phonon assistance. The phonon-assisted transitions provide a unique opportunity to investigate high excited states of the magneto-Coulomb system, which imitates the hydrogen atom in gigantic magnetic fields. High resolution data also reveal the presence of excited state magneto-donor transitions unknown until present.

[Contact: David G. Seiler, (301) 975-2074]

**SIGNALS & SYSTEMS METROLOGY PROGRAM****FAST SIGNAL ACQUISITION, PROCESSING, AND TRANSMISSION**Waveform Metrology

Released for Publication

Gans, W.L., **Dynamic Calibration of Oscilloscopes and Waveform Recorders Using Pulse Standards**, to be published in the Proceedings of the IEEE Instrumentation and Measurement Technology Conference, San Jose, California, February 13-15, 1990.

The purpose of this presentation is to convince the reader/listener of two key points. The first is that virtually no one calibrates oscilloscopes/waveform recorders properly and completely at present. The second is that, in most cases, the tools are now available to perform these complete and proper calibrations when the application requires it. After a brief introduction describing the current methods used to calibrate oscilloscopes, the problems associated with these methods are discussed and illustrated. The solutions to these problems are then described.

[Contact: William L. Gans, (303) 497-3538]

DC & Low Frequency Metrology

Released for Publication

Burroughs, C.J., and Hamilton, C.A., **Voltage Calibration Systems Utilizing Josephson Junction Arrays**, to be published in the Proceedings of the IEEE Instrumentation and Measurement Technology Conference, San Jose, California, February 13-15, 1990.

The recent development of large arrays of Josephson junctions is allowing an ever-increasing number of laboratories to maintain intrinsic Josephson voltage standards at an accuracy level near 0.05 ppm. This paper reviews the fundamentals of Josephson voltage standards and shows how computer control makes these standards simple to use in a variety of applications.

[Contact: Charles J. Burroughs, (303) 497-3901]

**Hamilton, C.A., Voltage Standard Devices.**

This article reviews the definition of the unit of voltage and the means by which arrays of Josephson junctions are used to implement that definition. The theory, design, and operation of Josephson array voltage standards are described.

[Contact: Clark A. Hamilton, (303) 497-3740]

**Hamilton, C.A., Burroughs, C.J., and Chieh, K., Operation of Josephson-Array Voltage Standards.**

This paper begins with a brief discussion of the physical principles and history of Josephson voltage standards. The main body of the paper deals with the practical details of the array design, cryoprobe construction, bias source requirements, adjustment of the system for optimum performance, calibration algorithms, and an assessment of error sources.

[Contact: Clark A. Hamilton, (303) 497-3740]

DC & Low Frequency Metrology (cont'd.)

## Recently Published

Hamilton, C.A., Lloyd, F.L., Chieh, K., and Goeke, W.C., A 10-V Josephson Voltage Standard, IEEE Transactions on Instrumentation and Measurement, Vol. 38, No. 2, pp. 314-316 (April 1989).

This paper describes the design and operation of an 18992 Josephson-junction array which can generate reference voltages up to 12 V. This device has applications for the direct calibration of Zener reference standards, calibrators, and digital voltmeters at the 10-V level, and for very accurate linearity and ratio measurements.

[Contact: Clark A. Hamilton, (303) 497-3740/3988]

Fundamental Electrical Measurements

## Recently Published

Cage, M.E., Semiclassical Scattering Corrections to the Quantum Hall Effect Conductivity and Resistivity Tensors, Journal Phys.: Condens. Matter, Vol. 1, No. 32, pp. 5531-5534 (1989).

Ando, Matsumoto, and Uemura published an important paper in 1975 that greatly influenced the early experimental work on the quantum Hall effect. Their paper showed that, in both a semiclassical scattering model and in a self-consistent Born approximation, there is a correction to the quantum Hall conductivity component  $\sigma_{xy}$  of the conductivity tensor that is directly proportional to the diagonal conductivity component  $\sigma_{xx}$ . We provide a detailed derivation of their results using the semiclassical scattering (relaxation-time approximation) model. We then present the surprising result that, in the semiclassical scattering model, there is no correction to the quantum Hall resistivity tensor component  $\rho_{xy}$  due to a finite value of  $\rho_{xx}$ .

[Contact: Marvin E. Cage, (301) 975-4248]

Cryoelectronic Metrology

## Released for Publication

Burroughs, C.J., and Hamilton, C.A., Voltage Calibration Systems Utilizing Josephson Junction Arrays, to be published in the Proceedings of the IEEE Instrumentation and Measurement Technology Conference, San Jose, California, February 13-15, 1990.

The recent development of large arrays of Josephson junctions is allowing an ever-increasing number of laboratories to maintain intrinsic Josephson voltage standards at an accuracy level near 0.05 ppm. This paper reviews the fundamentals of Josephson voltage standards and shows how computer control makes these standards simple to use in a variety of applications.

[Contact: Charles J. Burroughs, (303) 497-3901]

Gabutti, A., Gray, K.E., Wagner, R.G., and Ono, R.H., Granular-Aluminum Superconducting Detector for 6 keV X-rays and 2.2 MeV Beta Sources.

A 2- $\mu\text{m}$  superconducting strip of granular aluminum was used to detect the superconducting-to-normal transitions induced by the absorption of  $^{55}\text{Fe}$ , 6-keV X-rays, or the passage of electrons from a  $^{90}\text{Sr}$ , 2.2-MeV beta source. The count-rate for X-rays reaches almost 70% efficiency over a wide range of bias currents, confirming the potential application for high-spatial-resolution X-ray detectors. We report the first evidence of switching by a 2.2-MeV beta source which emits electrons in the minimum-ionizing range. However, the inability to distinguish between transitions caused by minimum-ionizing electrons emitted by the source prevented us from demonstrating the full sensitivity of the granular aluminum detector to minimum-ionizing radiation. The switching threshold for X-rays depends on thermal propagation of a normal region which bridges the film width, and a numerical simulation is

Cryoelectronic Metrology (cont'd.)

presented, the simple formulation of which allows extrapolation to other materials and temperatures. The very fast rise-time voltages are accurately described by a thermal propagation model.

[Contact: Ronald H. Ono, (303) 497-3762]

**Hamilton, C.A., Voltage Standard Devices.**

This article reviews the definition of the unit of voltage and the means by which arrays of Josephson junctions are used to implement that definition. The theory, design, and operation of Josephson array voltage standards are described.

[Contact: Clark A. Hamilton, (303) 497-3740]

**Hamilton, C.A., Burroughs, C.J., and Chieh, K., Operation of Josephson-Array Voltage Standards.**

This paper begins with a brief discussion of the physical principles and history of Josephson voltage standards. The main body of the paper deals with the practical details of the array design, cryoprobe construction, bias source requirements, adjustment of the system for optimum performance, calibration algorithms, and an assessment of error sources.

[Contact: Clark A. Hamilton, (303) 497-3740]

**Hu, Q., Mears, C.A., Richards, P.L., and Lloyd, F.L., Observation of Quantum Susceptance in Superconducting Tunnel Junctions.**

We have made the first direct measurement of the quantum susceptance which arises from the reactive part of quasi-particle tunneling in a superconductor-insulator-superconductor junction. The junction is coupled to an antenna and a superconducting microstrip stub to form a resonator; the resonant frequency is

measured from the response of the junction to broadband radiation from a Fourier transform spectrometer. A 19% shift of the resonant frequency, from 73 GHz to 87 GHz, is observed that arises from the change of the quantum susceptance of the junction with dc bias voltage. This shift is in excellent agreement with Werthamer-Tucker theory, which includes the quantum susceptance. This quantum susceptance should exist in all tunnel devices whose nonlinear I-V characteristics are due to elastic tunneling.

[Contact: Richard E. Harris, (303) 497-3776]

Recently Published

**Hamilton, C.A., Lloyd, F.L., Chieh, K., and Goeke, W.C., A 10-V Josephson Voltage Standard, IEEE Transactions on Instrumentation and Measurement, Vol. 38, No. 2, pp. 314-316 (April 1989).**

This paper describes the design and operation of an 18992 Josephson-junction array which can generate reference voltages up to 12 V. This device has applications for the direct calibration of Zener reference standards, calibrators, and digital voltmeters at the 10-V level, and for very accurate linearity and ratio measurements.

[Contact: Clark A. Hamilton, (303) 497-3740/3988]

**Hamilton, C.A., McDonald, D.G., Sauvageau, J.E., and Whiteley, S., Standards and High Speed Instrumentation, Proceedings of the IEEE, Vol. 77, No. 8, pp. 1224-1232 (August 1989).**

This paper reviews four applications of superconductivity which are of current interest in the field of metrology. These applications are Josephson series-array voltage standards, cryogenic current comparators, a superconducting sampling oscilloscope, and a new bolometer based on a kinetic inductance thermometer.

[Contact: Clark A. Hamilton, (303) 497-3740]

Antenna Metrology

Released for Publication

Francis, M.H., Kremer, D.P., and Repjar, A.G., **Antenna Measurements at Millimeter Frequencies.**

In the past, few antenna measurements above 30 GHz have been made by the National Institute of Standards and Technology (NIST). Recently, NIST has developed the capability to make antenna measurements at frequencies from 30 to 65 GHz. The extrapolation technique is used to determine the gain and polarization properties of antennas and probes with gains up to about 30 dB. The planar near-field technique is used for antennas with higher gains as well as for determining far-field antenna patterns for frequencies up to 50 GHz. This report describes the problems and the solutions for providing measurement capability at these frequencies. The problems that arise are primarily due to the small wavelengths at these frequencies requiring: (1) much better accuracies in the manufacture of flanges, (2) an improved technique for making insertion loss measurements, and (3) improved probe-positioning accuracy. [Contact: Michael H. Francis, (303) 497-5873]

Kremer, D.P., and Newell, A.C., **Millimeter Waveguide Alignment Fixture.**

Millimeter-wave measurements require that care be exercised in the connection and handling of the waveguide flanges and their contact surfaces. When properly connected, these flanges can provide many years of reliable and repeatable measurements. Improper use will limit the flange use to just a few connections and result in large measurement errors. These errors are especially acute in situations requiring repeated connecting and disconnecting of these flanges, such as in antenna or insertion loss measurement. Several factors contribute to these errors but the largest are: improperly installed

waveguide flanges, misalignment in flange connections, and excess strain on the waveguide or the flange.

The National Institute of Standards and Technology has addressed these problems by developing a mechanical alignment fixture for the millimeter-band waveguide. Two fixtures were developed: one for small devices such as standard-gain horns which can be supported by the fixture and another for larger devices. These systems, along with a properly installed flange, can reduce the uncertainty of the connection from greater than 1 dB to a few hundredths of a decibel.

[Contact: Douglas P. Kremer, (303) 497-3732]

Newell, A.C., **Development of Near-Field Test Procedures for Communication Satellite Antennas -- Phase II**, to be published as NISTIR 89-3930.

The results of near-field measurements on two antennas are described. The primary purpose for these measurements was the demonstration of measurement concepts developed during the first phase of this program. These measurements demonstrated the accuracy of beam pointing, gain and pattern data, swept near-field techniques, and diagnostic procedures for determining reflector shape.

[Contact: Allen C. Newell, (303) 497-3743]

Wittmann, R.C., **Spherical Near-Field Scanning: Determining the Incident Field Near a Rotatable Probe**, to be published in the Proceedings of the International Symposium on Antennas and Propagation, Dallas, Texas, May 7-11, 1990.

Many radar cross-section, electromagnetic interference/electromagnetic compatibility, and antenna measurements require a known incident field within a test volume. To evaluate systems designed to produce a specific incident field (compact ranges, for example), we

Antenna Metrology (cont'd.)

must measure the actual illumination for comparison with design specifications. Beyond its diagnostic value, these incident field data can also be used for error estimation and for calculating first-order corrections.

In this paper, we develop a spherical near-field scanning algorithm for determining incident fields inside a probe's "minimum sphere." This differs from the well-known spherical near-field scanning formulation which determines fields outside the source's minimum sphere. The scanner size depends on the extent of the region of interest and not on the extent of the (possibly much larger) source. The data may be collected using a standard roll-over-azimuth positioner.

[Contact: Ronald C. Wittmann, (303) 497-2236]

## Recently Published

Francis, M.H., **Antenna Far-Field Pattern Accuracies at Millimeter Wave Frequencies Using the Planar Near-Field Technique**, Proceedings of the Eleventh Annual Meeting and Symposium of the Antenna Measurement Techniques Association, Monterey, California, October 9-13, 1989, pp. 11-16 to 11-21.

In recent years there has been an increasing demand for antenna calibrations at millimeter-wave frequencies. Because of this, the National Institute of Standards and Technology (NIST) has been developing measurement capabilities at millimeter-wave frequencies. The development of gain and polarization measurement capabilities has been previously reported. This paper reports on the development of the capability to measure an antenna pattern which has been achieved during the last year. Measurement accuracies of better than 4 dB have been achieved for sidelobes which are 40 dB below the mainbeam peak. NIST is now providing a new measurement service for antenna patterns in the 30-

to 50-GHz frequency range.

[Contact: Michael H. Francis, (303) 497-5873]

Guerrieri, J.R., and Kremer, D.P., **Automated Multi-Axis Motor Controller and Data Acquisition System for Near-Field Scanners**, Proceedings of the Eleventh Annual Meeting and Symposium of the Antenna Measurement Techniques Association, Monterey, California, October 9-13, 1989, pp. 12-24 to 12-28.

The National Institute of Standards and Technology (NIST) has developed a multi-axis controller and software data acquisition system that has improved probe position accuracies in near-field scanning. This extends the usefulness of the NIST planar near-field scanner to higher frequencies. This system integrates programmable power supplies into an existing planar measurement system with new software that controls the power supplies and the data acquisition. It provides the higher positioning accuracy required for millimeter-wave measurements at a reasonable cost.

This system uses the NIST planar near-field scanner's existing dc motors, computer, and laser. The programmable power supplies are connected to the motors, with a separate power supply for each motor's armature and a common power supply for each of the motor's field windings. This allows for concurrent movement in each axis and eliminates delays in switching between axes. Directional control, motor protection, and special software features are implemented by logic control.

[Contact: Jeffrey R. Guerrieri, (303) 497-3863]

Muth, L.A., and Lewis, R.L., **Iterative Technique to Correct Probe Position Errors in Planar Near-Field to Far-Field Transformations**, Proceedings of the 1989 International Symposium on Antennas and Propagation, Tokyo, Japan, August 22-25, 1989, Vol. 4, pp. 901-904. [Also published as NIST

Antenna Metrology (cont'd.)

Technical Note 1323 (October 1988)].

We have developed a general theoretical procedure to take into account probe position errors when planar near-field data are transformed to the far field. If the probe position errors are known, we can represent the measured data as a Taylor series, whose terms contain the error function and the ideal spectrum of the antenna. Then we can solve for the ideal spectrum in terms of the measured data and the measured position errors by inverting the Taylor series. This is complicated by the fact that the derivatives of the ideal data are unknown; that is, they can only be approximated by the derivatives of the measured data. This introduces additional computational errors, which must be properly taken into account. We have shown that the first few terms of the inversion can be easily obtained by simple approximation techniques, where the order of the approximation is easily specified. A more general solution can also be written by formulating the problem as an integral equation and using the method of successive approximations to obtain a general solution. An important criterion that emerges from the condition of convergence of the solution to the integral equation is that the total averaged position error must be less than some fraction of the sampling criterion for the antenna under test.

[Contact: Lorant A. Muth, (303) 497-3703]

Muth, L.A., and Lewis, R.L., **Planar Near-Field Codes for Personal Computers**, NISTIR 89-3929 (October 1989).

We have developed planar near-field codes, written in FORTRAN, to serve as a research tool in antenna metrology. We describe some of the inner workings of the codes, the data management schemes, and the structure of the input/output sections to enable scientists and programmers to use these codes effec-

tively. The structure of the codes is seen to be open, so that a user should be able to incorporate a new application into the package for future use with relative ease. The large number of subroutines currently in existence are briefly described, and a table showing the interdependence among these subroutines is constructed. Some basic research problems, such as transformation of a near-field to the far-field and probe position error correction, are carried out from start to finish, to illustrate use and effectiveness of these codes. Sample outputs are shown. The advantage of a high degree of modularization is demonstrated by the use of disk-operating-system (DOS) batch files to execute FORTRAN modules in a desired sequence.

[Contact: Lorant A. Muth, (303) 497-3603]

Newell, A.C., Guerrieri, J.R., Persinger, R.R., Stiles, J.A., and McFarlane, E.J., **Comparison of Antenna Boresight Measurements Between Near-Field and Far-Field Ranges**, Proceedings of the Eleventh Annual Meeting and Symposium of the Antenna Measurement Techniques Association, Monterey, California, October 9-13, 1989, pp. 1-24 to 1-29.

This paper describes the results of electrical boresight measurement comparisons between one far-field and two near-field ranges. Details are given about the near-field alignment procedures and the near-field error analysis. Details of the far-field measurements and its associated errors are not described here, since the near-field technique is of primary interest. The coordinate systems of the antenna under test and the measurement ranges were carefully defined, and extreme care was taken in the angular alignment of each. The electrical boresight direction of the main beam was determined at a number of frequencies for two antenna ports with orthogonal polarizations. Results demonstrated a maximum uncertainty between the different ranges

Antenna Metrology (cont'd.)

of 0.018 degrees. An analytical error analysis that predicted a similar level of uncertainty was also performed. This error analysis can serve as the basis for estimating uncertainty in other near-field measurements of antenna boresight.

[Contact: Allen C. Newell, (303) 497-3743]

Newell, A.C., Kremer, D.P., and Guerrieri, J.R., **Improvements in Polarization Measurements of Circularly Polarized Antennas**, Proceedings of the Eleventh Annual Meeting and Symposium of the Antenna Measurement Techniques Association, Monterey, California, October 9-13, 1989, pp. 1-30 to 1-36.

A new measurement technique that is used to measure the polarization properties of dual-port, circularly polarized antennas is described. A three-antenna technique is used, and high-accuracy results are obtained for all three antennas without assuming ideal or identical properties. This technique eliminates the need for a rotating linear antenna, reduces the setup time when gain measurements are also performed, and reduces error for antennas with low axial ratios.

[Contact: Allen C. Newell, (303) 497-3743]

Microwave & Millimeter-Wave Metrology

Released for Publication

Holt, D.R., **Determination of Scattering Parameters with Respect to the Characteristic Impedance of Precision Coaxial Air-Line Standards**, to be published in the 1990 Conference on Precision Electromagnetic Measurements (CPEM) Digest, Ottawa, Canada, June 11-14, 1990.

Scattering parameter expressions with respect to the characteristic impedances in correspondence to the principal mode are developed for the coaxial air-line

standard. Dimensional variations of the inner and outer conductors and skin effect loss are included in the model. The local characteristic impedance, which is found from the stored energy principle, is derived from the forward and backward voltage and current waves of the principal mode. Four sources of error for  $|S_{11}|$  are discussed.

[Contact: Donald R. Holt, (303) 497-3574]

Kremer, D.P., and Newell, A.C., **Millimeter Waveguide Alignment Fixture.**

Millimeter-wave measurements require that care be exercised in the connection and handling of the waveguide flanges and their contact surfaces. When properly connected, these flanges can provide many years of reliable and repeatable measurements. Improper use will limit the flange use to just a few connections and result in large measurement errors. These errors are especially acute in situations requiring repeated connecting and disconnecting of these flanges, such as in antenna or insertion loss measurement. Several factors contribute to these errors but the largest are: improperly installed waveguide flanges, misalignment in flange connections, and excess strain on the waveguide or the flange.

The National Institute of Standards and Technology has addressed these problems by developing a mechanical alignment fixture for the millimeter-band waveguide. Two fixtures were developed: one for small devices such as standard-gain horns which can be supported by the fixture and another for larger devices. These systems, along with a properly installed flange, can reduce the uncertainty of the connection from greater than 1 dB to a few hundredths of a decibel.

[Contact: Douglas P. Kremer, (303) 497-3732]

Marks, R.B., and Phillips, K.R., **Wafer-Level ANA Calibrations at NIST**, to be published in the 34th Automatic RF

Microwave & Millimeter-Wave (cont'd.)

Techniques Group (ARFTG) Conference Digest, Dallas, Texas, May 10-11, 1990.

The National Institute of Standards and Technology (NIST) program supporting on-wafer S-Parameter measurements seeks to transfer methodology and software to industrial measurement laboratories. The subject of this paper is the development of calibration techniques and algorithms rather than physical standards. In particular, we discuss a method based on the through-reflect-line technique. This method uses transmission lines as standards; it also incorporates redundant measurements to improve calibration accuracy and bandwidth.

[Contact: Roger B. Marks, (303) 497-3037]

Williams, D.F., **Development of On-Wafer Microwave Standards at NIST**, to be published in the 34th Automatic RF Techniques Group (ARFTG) Conference Digest, Dallas, Texas, May 10-11, 1990.

The National Institute of Standards and Technology (NIST) has begun a program to develop standards and calibration services for microwave wafer-level probing systems. The program objectives, organization, and plans are discussed.

[Contact: Dylan F. Williams, (303) 497-3138]

## Recently Published

Adair, R.T., and Livingston, E.M., **Coaxial Intrinsic Impedance Standards**, NIST Technical Note 1333 (October 1989).

This paper discusses how impedance standards are derived from the basic definition of impedance, constructed, and used in metrology with coaxial air-line systems. Basic transmission line equations are reviewed with emphasis given to intrinsic or derived standards

for obtaining the impedance in low-loss transmission line systems. A brief description is given of how impedance standards are used to calibrate the vector automatic network analyzer, and specifically, the six-port system automatic network analyzer used at the National Institute of Standards and Technology (NIST) for calibration services in the radio-frequency, microwave, and millimeter-wave areas. Measurement uncertainties are given for 7-mm coaxial devices measured with the NIST six-port system. The resolution of this six-port system is several orders more precise than that of the present impedance standards from which it is calibrated. Required improvements in the physical dimensions of air-line standards which permit the capability of the automatic network analyzer to be more fully utilized are given.

[Contact: John R. Juroshek, (303) 497-5362]

Hoer, C.A., **Systematic Errors in Power Measurements Made With a Dual Six-Port ANA**, NIST Technical Note 1332 (July 1989).

The purpose of this report is to determine the systematic error in measuring power with a dual six-port automatic network analyzer (ANA). Most of the report concentrates on developing equations for estimating systematic errors due to imperfections in the test port connector, imperfections in the connector on the power standard, and imperfections in the impedance standards used to calibrate the six-port for measuring reflection coefficient. These are the largest sources of error associated with the six-port. For 7-mm connectors, all systematic errors which are associated with the six-port add up to a worst-case uncertainty of  $\pm 0.00084$  in measuring the ratio of the effective efficiency of a bolometric power sensor relative to that of a standard power sensor.

[Contact: David H. Russell, (303) 497-3148]

Optical Fiber Metrology

Released for Publication

Franzen, D.L., **Measurement Standards to Support Photonics Technology**, to be published in the Proceedings of the IEEE Instrumentation Measurement Technology Conference, San Jose, California, February 13-15, 1990.

Standards to support the emerging photonics/lightwave technology industry can be classified into two groups: physical primary standards maintained by national standards laboratories and standard measurement procedures agreed upon by domestic and international voluntary standards bodies. The measurement of absolute optical power leads the prioritized list of primary standards needs. The progress at the National Institute of Standards and Technology (NIST) toward the development and distribution of optical power and other primary standards is reviewed. Standard measurement procedures to characterize fiber, cables, sources, detectors, and lightwave systems have been the focus of domestic and international standards bodies for the past decade. The interaction between NIST and these standards groups to evaluate the precision and accuracy of several test methods is reported. In some cases, the evaluations resulted in technical changes to commonly accepted practices.

[Contact: Douglas L. Franzen, (303) 497-3346]

Recently Published

Danielson, B.L., and Whittenberg, C.D., **Group Index and Time Delay Measurements of a Standard Reference Fiber**, NISTIR 88-3091 (July 1988).

We describe measurement techniques for establishing a standard reference fiber with a well-characterized group index and time or group delay. Evaluation of an interferometric method indicates that fiber group index can be determined

with a total estimated uncertainty of about 0.03% in small samples. Group delay of the reference fiber was measured with an overall uncertainty less than 0.004% in a 7-km waveguide. We discuss the application of a standard reference fiber to calibration of the distance measurement accuracy of an optical time-domain reflectometer.

[Contact: Bruce L. Danielson, (303) 497-5620]

Electro-Optic Metrology

Released for Publication

Franzen, D.L., **Measurement Standards to Support Photonics Technology**, to be published in the Proceedings of the IEEE Instrumentation Measurement Technology Conference, San Jose, California, February 13-15, 1990.

Standards to support the emerging photonics/lightwave technology industry can be classified into two groups: physical primary standards maintained by national standards laboratories and standard measurement procedures agreed upon by domestic and international voluntary standards bodies. The measurement of absolute optical power leads the prioritized list of primary standards needs. The progress at the National Institute of Standards and Technology (NIST) toward the development and distribution of optical power and other primary standards is reviewed. Standard measurement procedures to characterize fiber, cables, sources, detectors, and lightwave systems have been the focus of domestic and international standards bodies for the past decade. The interaction between NIST and these standards groups to evaluate the precision and accuracy of several test methods is reported. In some cases, the evaluations resulted in technical changes to commonly accepted practices.

[Contact: Douglas L. Franzen, (303) 497-3346]

Goyal, I.C., Gallawa, R.L., and Ghatak,

Electro-Optic Metrology (cont'd.)**A.K., An Approximate Solution to the Scalar Wave Equation for Planar Optical Waveguides.**

We consider an approximate solution to the one-dimensional scalar wave equation appropriate to the planar optical waveguides often encountered in practice. The refractive index profile may be arbitrary. The method described here is more accurate and useful than the WKB method, which has often been applied to problems of this type, as unlike the WKB method, this method is valid even at turning points (WKB refers to the initials of three independent workers -- Wentzel, Kramers, Brillouin -- who first used the approximation procedure to solve the Schroedinger wave equation in one dimension). The fields and the propagation constants for the lowest order modes for two profiles are calculated and compared with the exact solution.

[Contact: Robert L. Gallawa, (303) 497-3761]

Sanford, N.A., Hickernell, R.K., and Craig, R.M., **Photorefractive Instabilities in Proton-Exchanged Two-Wave Coupling and Chaos**, to be published in the Proceedings of the 1990 Integrated Photonics Research Conference, Hilton Head, South Carolina, March 26-28, 1990.

Forward and self-seeded backward waves in proton-exchanged waveguides exhibit repetitive transient coupling with a threshold of tens of milliwatts at 1064 nm. A time series of the quasi-periodic coupling suggests intermittency as a route to chaos.

[Contact: Norman A. Sanford, (303) 497-5239]

Sanford, N.A., Malone, K.J., and Larson, D.R., **An Integrated Optic Laser Fabricated by Field-Assisted Ion-Exchange in Neodymium-Doped Soda-Lime Silicate Glass**, to be published in the Proceedings of the 1990 Integrated

Photonics Research Conference, Hilton Head, South Carolina, March 26-28, 1990.

A continuous-wave channel waveguide laser operating at 1057 nm has been fabricated in neodymium-doped soda-lime silicate glass by field-assisted ion exchange. Threshold for pumping at 528 nm is 31 mW. Slope efficiency is 0.5%. [Contact: Norman A. Sanford, (303) 497-5239]

## Recently Published

Deeter, M.N., Rose, A.H., and Day, G.W., **Characteristics of Polarimetric Magnetic Field Sensors Based on Yttrium Iron Garnet**, Conference Digest of the 1989 LEOS (IEEE Lasers and Electro-Optics Society) Meeting, Orlando, Florida, October 17-20, 1989, Vol. M7.3, p. 110.

We describe the performance characteristics of polarimetric Faraday-effect magnetic field sensors employing ferrimagnetic-sensing elements, such as yttrium iron garnet (YIG). Experimental results of sensor sensitivity, linearity, and directionality are presented for three cylindrical YIG samples, each having a different length-to-width ratio.

[Contact: Merritt N. Deeter, (303) 497-5400]

Gallawa, R.L., and Tu, Y., **Analysis of Circular Bends in Planar Optical Waveguides**, Fiber and Integrated Optics, Vol. 8, pp. 87-97 (November 21, 1988).

Waveguides with circular bends are analyzed by means of a conformal transformation in conjunction with the WKB method of dealing with the non-uniform refractive index that results from the transformation. The result is a prediction of the operational parameters of the bent guide, including the loss. The transformation makes possible an intuitive understanding of the cause of the loss.

Electro-Optic Metrology (cont'd.)

[Contact: Robert L. Gallawa, (303) 497-3761]

Lee, K.S., **New Compensation Method for Bulk Optical Sensors with Multiple Birefringences**, Applied Optics, Vol. 28, No. 11, pp. 2001-2011 (1 June 1989).

The dielectric tensor of an anisotropic crystal with multiple perturbations is presented to include the effects of multiple perturbations. To study electromagnetic wave propagation in anisotropic crystals subject to various influences, the perturbed dielectric tensor is substituted into Maxwell's equation. Then, a 2 x 2 transmission matrix formalism, based on a normal-mode approach, is extended to anisotropic crystals possessing multiple birefringences to develop compensation schemes for ac optical sensors employing the crystal. It is shown that a new compensation method utilizing two analyzers can eliminate the effects of both unwanted linear birefringences and unwanted circular birefringences on the stability of the ac bulk polarimetric optical sensor. The conditions (here referred to as the quenching conditions) in which the compensation method becomes important are also derived for both voltage (or electric field) and current (or magnetic field) sensors.

[Contact: G. W. Day, (303) 497-5204]

Rasmussen, A.L., Simpson, P.A., and Sanders, A.A., **Improved Low-Level Silicon-Avalanche-Photodiode Transfer Standards at 1.064 Micrometers**, NISTIR 89-3917 (August 1989).

Three silicon-avalanche-photodiode transfer standards (APD TS) were calibrated from  $\approx 10^{-8}$  to  $\sim 10^{-5}$  W/cm<sup>2</sup> peak power density at approximately 10% uncertainty. Calibrations were performed for 1.064- $\mu$ m wavelength pulses, having 10- to 100-ns durations. For this calibration, an acousto-optically modulated laser beam provided

alternately equal levels of pulsed power and cw power into a low-level beam splitter. The cw power measured by a transfer standard in the transmitted beam of the splitter was used to determine the pulsed power into the APD transfer standard in one of the low-level reflected beams of the splitter. The APD detector had about 1-cm<sup>2</sup> aperture and a 3.8-cm focal length lens in front of it. Lens, window, and detector surfaces had narrow-band anti-reflection coatings. The commercial detector package is a temperature-compensated, infrared-enhanced APD preamplifier module. To increase the sensitivity, one or two 20-dB, 500-MHz band-width amplifiers followed the preamplifier. At very low pulsed power levels, a 30-MHz low-pass filter with gaussian roll-off was attached to the amplifier output to reduce the noise. A transient digitizer recorded the impulse responses of the APD detectors at 1.064  $\mu$ m. These data were read into computer programs that convolved the unity area impulse response with unity height gaussian pulses. From these data, correction factors of the pulse peak for observed pulse durations from 10 to 100 ns were determined. Instructions, calibrations, error budgets, and system descriptions are included.

[Contact: Alvin L. Rasmussen, (303) 497-5367]

Schlager, J.B., Yamabayashi, Y., and Franzen, D.L., **Soliton-Like Compression of Pulses from Erbium-Fiber Lasers**, Proceedings of the European Conference on Optical Communications, Gotenburg, Sweden, September 10-14, 1989, Vol. 3, pp. 62-65.

Erbium-fiber lasers with cavity lengths of 5 to 5000 m are mode-locked at the fundamental cavity frequency. Pulse durations vary from 13 to 80 ps; the shorter pulses exhibit soliton-like compression and higher order effects when propagated through external fibers. [Contact: John B. Schlager, (303) 497-3542]

Electro-Optic Metrology (cont'd.)

Schlager, J.B., Yamabayashi, Y., Franzen, D., and Juneau, R.I., **Mode-Locked, Long-Cavity, Erbium Fiber Lasers with Subsequent Soliton-Like Compression**, IEEE Photonics Technology Letters, Vol. 1, No. 9, pp. 264-266 (September 1989).

Erbium fiber lasers with cavity lengths of 20 to 5000 m are mode-locked at the fundamental cavity frequency using an integrated-optic intensity modulator driven by a novel pulse generator. Resulting optical pulses at 1536 nm are recorded with a synchroscan streak camera and have durations of 18 to 80 ps with peak powers over 6 W. The shorter cavities yield nearly transform-limited pulses which are narrowed by soliton-like compression to approximately 5 ps after propagation through an external 14-km fiber.

[Contact: John B. Schlager, (303) 497-3542]

Electromagnetic Properties

Released for Publication

Geyer, R.G., **Electrodynamics of Materials for Dielectric Measurement Standardization.**

Dielectric reference materials are analyzed in light of the fundamental requirements of linearity, homogeneity, and isotropy. Generalized frequency- and temperature-dependent dispersion relations are reviewed which allow the prediction of broadband dielectric behavior from limited measurement data, determination of valid modal field structure in cavity or waveguide fixtures, and identification of discrepancies and errors in measurement data. An approach for examining the influence of deviations of sample homogeneity on a precisely specified electromagnetic field structure is outlined, and sufficient conditions for isotropic or uniaxial or biaxial anisotropic dielectric behavior are

examined in terms of a material's chemical lattice physics. These characteristics direct the choices of suitable reference materials useful in dielectric metrology. Lastly, advances at the National Institute of Standards and Technology in both transmission/reflection and cavity resonator measurement techniques incorporating dielectric reference materials are noted.

[Contact: Richard G. Geyer, (303) 497-5852]

## Recently Published

Kremer, D.P., Newell, A.C., and Agee, D.A., **Absorber Characterization**, Proceedings of the Eleventh Annual Meeting and Symposium of the Antenna Measurement Techniques Association, Monterey, California, October 9-13, 1989, pp. 13-7 to 13-11.

When a laboratory considers replacing an old microwave absorber or a new installation, it needs a method that makes possible quick, inexpensive, and accurate measurements on individual absorber samples. Different types and sizes of absorber need to be quickly analyzed at multiple frequencies to determine which type best maintains or improves the facility's radio-frequency characteristics. In response to this need, the National Institute of Standards and Technology has devised an improved version of the Doppler-shift method to measure the scattering levels of different sizes and types of microwave absorber. This technique is useful as an inexpensive and simple method for measuring individual absorber pieces with good accuracy and sensitivity. The system described does not require a large anechoic facility or a sophisticated measurement system for minimizing the effects of background scattering. Using this method, reflectivity levels on the order of -80 dB can be measured and relative changes of 1 dB can be detected. Sample results for an absorber with and without fire retardant salts and different sizes are presented.

Electromagnetic Properties (cont'd.)

[Contact: Douglas P. Kremer, (303) 497-3732]

Complex Testing

## Recently Published

Stenbakken, G.N., Souders, T.M., and Stewart, G.W., **Ambiguity Groups and Testability**, IEEE Transactions on Instrumentation and Measurement, Vol. 38, No. 5, pp. 941-947 (October 1989).

An efficient method has been developed for determining component ambiguity groups which arise in analog circuit testing. The method makes use of the sensitivity model of the circuit. The ambiguity groupings are shown to depend on the test points selected and the measurement accuracy, and is, therefore, a useful tool for determining where to add or delete test points. The concept of ambiguity groups can be used to refine the testability measure of a circuit.

[Contact: Gerard N. Stenbakken, (301) 975-2440]

Other Fast Signal Topics

## Released for Publication

Capobianco, T.E., **Using an Eddy Current Impedance Plane Display Instrument for Probe Characterization**, to be published in the Proceedings of the 38th Defense Conference on Nondestructive Testing (NDT), San Antonio, Texas, October 31-November 2, 1989.

The U.S. Army is sponsoring work at the National Institute of Standards and Technology to develop a military standard for characterizing the performance of eddy-current probes for nondestructive testing. Presently, the test method of this draft standard constitutes a measurement of the change in probe impedance when the probe is applied to test blocks of two different conductivities. It was hoped that this

impedance measurement would be easy to perform in the field, but we discovered that field- and depot-level operations lack the equipment for measuring impedance, a serious obstacle to the implementation of the standard. However, depot operations often have an eddy-current instrument which displays flaw signals in the impedance plane. These instruments do not display the actual impedance values for the flaw signals, but could possibly be calibrated for this purpose. Results are presented of an experiment where a calibration technique was tried and eddy-current probe impedances measured. The calibration technique consists of using a switchable combination of resistors and inductors to produce reference points on the display of the impedance-plane instrument. The impedance measurements were made by interpolating values from these reference points for flaw signals obtained when the probes were scanned over an electrical discharge machined notch in 6061-T651 aluminum.

[Contact: Thomas E. Capobianco, (303) 497-3141]

Fulcomer, P.M., **Prospects for the Use of Lithium Batteries in Law Enforcement Equipment**, to be published as a National Institute of Justice Technology Assessment Report.

Lithium batteries have been available for a number of years, mainly in primary type (nonrechargeable), low-current-drain configurations (i.e., less than 10 mA). Within the past several years, more medium-to-high-current drain (50 to 500 mA) lithium primary cells have become available, and within the past few years lithium secondary cells (rechargeable) have been introduced. The advantages of lithium include better low-temperature performance and much longer shelf life for primary cells, and superior charge retention and lack of a memory effect for secondary cells. Both types can provide significantly more power per volume and per weight than equivalent nonlithium batteries. In

Other Fast Signal Topics (cont'd.)

addition to the advantages and disadvantages of lithium batteries and their applicability for use in law enforcement equipment, this report discusses lithium battery background, the safety precautions required in the use of lithium cells, and the battery requirements for present law enforcement equipment. The report concludes that the use of lithium batteries would be beneficial to the operation of most battery-operated equipment used by law enforcement personnel. To fully realize the advantages mentioned above, however, and to minimize the effect of their higher initial cost, lithium batteries should, with two exceptions, be designed into new equipment.

[Contact: P. Michael Fulcomer, (301) 975-2407]

Hill, D.A., **Quasi-Static Analysis of a Two-Wire Transmission Line Located at an Interface.**

Simple quasi-static expressions have been derived for the propagation constant, the characteristic impedance, and the field distribution of a two-wire transmission line located at the air-earth interface. Both the complex permittivity and the complex permeability of the earth are allowed to differ from the free-space values, and a numerical solution of the mode equation shows that quasi-static approximation is valid when the wire separation is much less than a free-space wavelength. The quasi-static approximation can be used to determine both the complex permittivity and the complex permeability of the earth from measurements of the propagation constant and the characteristic impedance of the transmission line.

[Contact: David A. Hill, (303) 497-3472]

Recently Published

Haggerty, J., and Young, M., **Spatial Light Modulator for Texture Classifi-**

**cation**, Applied Optics, Vol. 28, No. 23 (1 December 1989).

This paper describes a hybrid computer-optical processor devoted to the analysis of texture. Textures are displayed on a spatial light modulator, and their power spectra are calculated optically by a Fourier optical technique. A video camera and a computer with a frame digitizer process the power spectra. We define a multidimensional feature space and associate each texture with a point in this feature space. After a training set, the system can distinguish several textures. This hybrid computer is a step toward real-time texture classification because of the nearly instantaneous optical Fourier transformation.

[Contact: Matt Young, (303) 497-3223]

Leedy, T.F., **NIST Developing Neutral Format for HMA Manufacturers**, Navy Manufacturing Technology Program Report, pp. 4-5 (November 1989).

The National Institute of Standards and Technology (NIST) Electricity Division of the Center for Electronics and Electrical Engineering and the NIST Automated Manufacturing Research Facility of the Center for Manufacturing Engineering have started a three-year program entitled, "A Data Format Specification for Hybrid Microelectronic Assemblies," sponsored by the Naval Ocean Systems Center, San Diego. The two centers are part of NIST. Project objective is to develop a specification for a neutral format to promote the exchange of design and manufacturing data for hybrid microcircuit assemblies. Comments from industry are being solicited at two special workshops.

[Contact: Thomas F. Leedy, (301) 975-2410]

Ramboz, J.D., **Special Test and Evaluation Methods Used for a Nine-Axis Accelerometer**, NISTIR 89-4195 (October 1989).

The test methods used to characterize

Other Fast Signal Topics (cont'd.)

and evaluate the performance of a miniature nine-axis accelerometer are discussed. A special transducer containing nine separate linear accelerometers was examined. The intended application for this type of device is to derive angular acceleration data for dynamic-head motion measurements relating to automobile crash studies. The accelerometers, amplifiers, multiplexer, FM telemetry transmitter, and power supply are all to be molded into an athletic orthodontic mouthpiece, and data will be obtained from measurements taken from boxers' head motions. The angular head motions of boxers is thought to be similar to those in automobile crashes. The transducer parameters tested include axial and transverse linear-vibration sensitivities, equivalent acceleration noise, effects of power supply voltage variations, and mouthpiece vibration transmissibility. Special test apparatus described includes a dual centrifuge and a dual spin-axis rate-table. Test philosophy and some test results are used to illustrate how apparently conflicting test results can be used to explain transducer performance under test conditions of combined environments.

[Contact: John D. Ramboz, (301) 975-2434]

Schoenwetter, H.K., Leedy, T.F., and Laug, O.B., **Electrical Performance Tests for Storage Oscilloscopes**, NISTIR 89-4220 (December 1989).

Electrical performance test procedures for a dc to 100-MHz storage oscilloscope were developed for the purpose of evaluating samples submitted by electronic instrument manufacturers in response to specifications issued by the U.S. Army Communications-Electronics Command. The detailed, step-by-step test procedures are based on the specifications supplied by the Army and include sample data sheets and tables for the recording of interim data and

final test results.

This report discusses the measurement principles and techniques underlying the most significant procedures. In addition, the sources of measurement uncertainty are discussed.

[Contact: Owen B. Laug, (301) 975-2412]

## ELECTRICAL SYSTEMS

Power Systems Metrology

Released for Publication

Kelley, E.F, and McKnight, R.H., **Streamer Propagation in Transformer Oil Under the Influence of Submicrosecond Rise-Time Pulses.**

The propagation of prebreakdown streamers in transformer oil is investigated for microsecond and submicrosecond pulses applied to a needle-sphere electrode geometry. For microsecond pulses, the streamer begins with a slower process. As the slow streamer crosses the gap, if a critical field is reached at the streamer's tip, a faster event completes the streamer's growth and leads to breakdown of the gap. As the voltage increases so that the streamer grows more quickly, the faster event is found to dominate that growth. Ultimately, under large overvoltage conditions, the slower event is barely visible, and breakdown occurs mostly by a fast streamer. Under the application of fast-rise pulses, a similar phenomenon is observed when the slow events are generated; however, once a critical voltage is reached, no slow event is produced, and the breakdown is completed via fast processes which increase their average speed as the voltage increases. For the system studied, it is possible to cause breakdown at a lower voltage with a fast-rise pulse than with a microsecond pulse only when the fast-rise pulse is compared with a microsecond pulse which greatly overstresses the gap.

[Contact: William E. Anderson, (301) 975-2423]

Power Systems Metrology (cont'd.)

Misakian, M., **An Evaluation of Instrumentation Used to Measure Power Line Magnetic Fields** [to be presented at the Power Engineering Society Meeting, Minneapolis, Minnesota, July 1990].

This report is part of an IEEE Power Engineering Society (PES) working group paper describing tests of power-frequency field measurement instrumentation performed during a "field day" held at the Bonneville Power Administration. The group in question is the AC Fields Working Group of the Corona and Fields Effects Subcommittee of the PES Transmission and Distribution Committee. [Contact: Martin Misakian, (301) 975-2426]

Misakian, M., **Measurements of Power-Frequency Magnetic Fields.**

Recent epidemiological studies have focused attention on the measurement of ambient-level power-frequency magnetic fields in residential and industrial settings. These fields can be as much as two orders of magnitude smaller than power-line magnetic fields and can also contain significant levels of harmonic content. Because the existing U.S. standard for characterizing power-frequency magnetic fields is intended for measurements near power lines, it has a number of inadequacies if used for guidance during the measurement of ambient fields. This paper describes the instrumentation and calibration procedures and outlines measurement strategies which can overcome some of the shortcomings of the existing standard. Examples of ambient-level magnetic field measurements are also provided. [Contact: Martin Misakian, (301) 975-2426]

Van Brunt, R.J., **Preface to book entitled, "Nonequilibrium Effects in Ion and Electron Transport (Sixth International Swarm Seminar)."**

This volume presents the contributions of the participants in the Sixth International Swarm Seminar, held August 2-5, 1989 at the Webb Institute in Glen Cove, New York. The Swarm Seminars are traditionally held as relatively small satellite conferences of the International Conference on the Physics of Electronic and Atomic Collisions (ICPEAC) which occurs every two years. The 1989 ICPEAC took place in New York City prior to the Swarm Seminar. The focus of the Swarm Seminars has been on basic research relevant to understanding the transport of charged particles, mainly electrons and ions, in weakly ionized gases. This is a field that tends to bridge the gap between studies of fundamental binary atomic and molecular collision processes and studies of electrical breakdown or discharge phenomena in gases. Topics included in the 1989 seminar ranged the gamut from direct determinations of charged-particle collision cross sections to use of cross sections and swarm parameters to model the behavior of electrical gas discharges. Although the range of subjects covered was in many respects similar to that of previous seminars, there was an emphasis on certain selected themes that tended to give this seminar a distinctly different flavor. There was, for example, considerable discussion on the meaning of "equilibrium" and the conditions under which nonequilibrium effects become important in the transport of electrons through a gas. It is evident from work presented here that under certain gas discharge or plasma conditions nonequilibrium effects can be significant; therefore, application of swarm or transport parameters determined under equilibrium conditions to the modeling of such discharges or plasmas must be considered questionable. The discussions at this seminar, as represented by several of the invited papers, has helped to remove some of the confusion about the applicability of equilibrium assumptions and provided guidance for attempts to deal with nonequilibrium situations. The seminar

Power Systems Metrology (cont'd.)

also included discussions about the meaning and determination of higher order "diffusion coefficients" in electron transport and limitations on the range of validity of "modified effective range theory." Interesting new developments on both topics were presented. Several of the invited papers were concerned with the peculiarities of ion transport in sulfur hexafluoride, a gas that has become increasingly important because of use in plasma processing of electronic materials and as a gaseous dielectric in electrical power systems. An attempt was made for the first time to include papers on electron transport in dense media, namely, high-pressure gases and liquids.

The 1989 Swarm Seminar was sponsored jointly by the Polytechnic University of New York, the National Institute of Standards and Technology, and the Naval Surface Warfare Center. Financial support for the seminar was also provided by the U.S. Air Force Office of Scientific Research.

[Contact: Richard J. Van Brunt, (301) 975-2425]

Van Brunt, R.J., and Herron, J.T., *Fundamental Processes of SF<sub>6</sub> Decomposition and Oxidation in Glow and Corona Discharges.*

The current state of our knowledge about the fundamental collision processes involving electrons, ions, free radicals, and molecules needed to understand the gas-phase discharge chemistry in SF<sub>6</sub> is reviewed. It is shown that the electron-impact dissociation of SF<sub>6</sub> leading to reactive neutral fragments is the decomposition-rate controlling factor in corona and glow discharges. Data on electron-impact cross sections for SF<sub>6</sub> are reviewed and used to compute SF<sub>6</sub> dissociation rates as functions of electric field-to-gas density ratios (E/N) for mixtures of SF<sub>6</sub> with O<sub>2</sub> and H<sub>2</sub>O. The calculated and

measured rates for subsequent gas-phase reactions involving the lower valence sulfur fluorides (SF<sub>x</sub>, x < 6) and other reactive species like OH and O are also reviewed. The temperature and E/N dependencies of rates for F<sup>-</sup> transfer reactions of SF<sub>6</sub><sup>-</sup> with SOF<sub>4</sub>, SO<sub>2</sub>, SiF<sub>4</sub>, and other species generated by discharge-induced oxidation of SF<sub>6</sub> are reviewed together with data on collisional electron detachment and ion conversion processes involving interactions of F<sup>-</sup>, SF<sub>5</sub><sup>-</sup>, and SF<sub>6</sub><sup>-</sup> with SF<sub>6</sub>. The relevance of these negative-ion molecule interactions to ion transport and oxidation rates in SF<sub>6</sub> is discussed. Rates for various slow gas-phase hydrolysis processes that can affect observed relative yields of oxidation by-products are also considered. Implications of the fundamental rate data reviewed here to recently proposed chemical kinetics models of corona and glow-type discharges in SF<sub>6</sub> are discussed.

[Contact: Richard J. Van Brunt, (301) 975-2425]

## Recently Published

Martzloff, F.D., and Leedy, T.F., *A Glimpse at Long-Term Effects of Momentary Overvoltages on Zinc Oxide Varistors*, Ceramic Transactions, Vol. 3, pp. 306-311 (1989), Proceedings of the Second International Varistor Conference, Schenectady, New York, December 4-5, 1988.

Because the prime function of varistors is diversion of high-energy surges, most of the attention is directed toward selecting the appropriate device rating to ensure long life under surge conditions. Some attention is also given to matching steady-state rating of the device to the power system voltage. However, during abnormal (and not well-defined) power system conditions, the line voltage can reach values that will cause substantial current in the varistor. Until the effects of these momentary overvoltages are better identified and understood, there will be

Power Systems Metrology (cont'd.)

a risk of near-term failure at worst and accelerated aging at best.

[Contact: Francois D. Martzloff, (301) 975-2409]

Misakian, M., and McKnight, R.H., **DC Electric Field Effects During Measurements of Monopolar Charge Density and Net Space Charge Density Near HVDC Power Lines**, IEEE Transactions on Power Delivery, Vol. 4, No. 4, pp. 2229-2234 (October 1989).

The influence of a dc electric field on the measurement of monopolar charge densities using an aspirator-type ion counter and the measurement of net space charge density using a Faraday cage or filter is examined. Optimum configurations which minimize the effect of the electric field are identified for each type of instrumentation.

[Contact: Martin Misakian, (301) 975-2426]

Pace, M.O., Wintenberg, A.L., Blalock, T.V., Kelley, E.F., FitzPatrick, G.J., Fenimore, C., and Yamashita, H., **Pressure Effects on Partial Discharges in Hexane Under DC Voltage**, 1989 Annual Report, Conference on Electrical Insulation and Dielectric Phenomena, Leesburg, Virginia, October 29-November 1, 1989, pp. 87-92 (1989).

The pressure dependencies of the early partial discharges (PD) have been experimentally investigated at a needle in hexane from subatmospheric pressure (near hexane vapor pressure) to several atmospheres. Each PD is photographed in synchronism with a characteristic pattern of current pulses. An image-preserving optical delay allows photography to commence just before or at inception. Individual current pulses comprising a characteristic pattern are resolved.

[Contact: Gerald J. FitzPatrick, (301) 975-2737]

Petersons, O., **Review of book entitled,**

**"The Current Comparator,"** by W.J.M., Moore and P.N. Miljanic, *Metrologia* (Journal published in France by the Bureau International des Poids et Mesures), Vol. 26, No. 1, pp. 77-78 (March 1989).

This review covers the book, "The Current Comparator," by W. J. M. Moore and P. N. Miljanic. The review includes an overall assessment of the coverage of the subject, and addresses the clarity and effectiveness of the authors in reaching their intended audience. The book is a concise, yet comprehensive monograph covering the basic principles, construction, details, error sources, and error reduction techniques for magnetic current comparators. Alternating- (power frequency) and direct-current comparators are covered. Numerous applications and instruments utilizing current comparators are described. The book serves both as tutorial material for the uninitiated and as a reference volume for the expert.

[Contact: Oskars Petersons, (301) 975-2400]

Van Brunt, R.J., **Research for Electric Energy Systems - An Annual Report**, NISTIR 89-4167 (October 1989).

This is a report of technical progress in four investigations conducted at the National Institute of Standards and Technology and supported by the U.S. Department of Energy under Task Order Number 137. The first investigation is concerned with the measurements of electric fields and ions in the vicinity of high-voltage transmission lines and biological exposure facilities. For this investigation, results are reported on evaluations of two methods for measuring ion mobilities at atmospheric pressure and an aspiratory-type ion counter for measuring monopolar charge densities in air. The second investigation is concerned with development of advanced diagnostics for compressed gas-insulated power systems. For this investigation, results are reported on

Power Systems Metrology (cont'd.)

measurements of collisional electron detachment and negative ion conversion reactions in  $SF_6$  and on a new technique for measuring the stochastic behavior of partial discharges. The third investigation is concerned with measurement of prebreakdown phenomena at solid-liquid dielectric interfaces. Results are presented here from optical observations of the influence of hydrostatic pressure on prebreakdown partial discharge development and measurement of nanosecond impulse breakdown at liquid-solid interfaces. The fourth area of research is concerned with electrical measurement of fast transient phenomena. Results are presented from an investigation into the interactions between two dividers used simultaneously to measure fast impulse voltages.

[Contact: Richard J. Van Brunt, (301) 975-2425]

Van Brunt, R.J., and Kulkarni, S.V., **Method for Measuring the Stochastic Properties of Corona and Partial-Discharge Pulses**, Review of Scientific Instruments, Vol. 60, No. 9, pp. 3012-3023 (September 1989).

A new method is described for measuring the stochastic behavior of corona and partial-discharge pulses which utilizes a pulse selection and sorting circuit in conjunction with a computer-controlled multichannel analyzer to directly measure various conditional and unconditional pulse-height and pulse-time-separation distributions. From these measured distributions it is possible to determine the degree of correlation between successive discharge pulses. Examples are given of results obtained from measurements on negative, point-to-plane (Trichel-type) corona pulses in an  $N_2/O_2$  gas mixture which clearly demonstrate that the phenomenon is inherently stochastic in the sense that development of a discharge pulse is significantly affected by the amplitude of and time separation from the

preceding pulse. It is found, for example, that corona discharge pulse amplitude and time separation from an earlier pulse are not independent random variables. Discussions are given about the limitations of the method, sources of error, and data analysis procedures required to determine self-consistency of the various measured distributions. [Contact: Richard J. Van Brunt, (301) 975-2425]

Superconductors

Released for Publication

Cross, R.W., and Goldfarb, R.B., **Variable Frequency Magnetometer for Superconductor Toroids.**

We constructed a flux-integration magnetometer and made magnetization measurements on a toroidal sample of a  $YBa_2Cu_3O_x$  high-critical-temperature superconductor as a function of magnetic field amplitude, frequency, and temperature. The toroid geometry gives calibrated hysteresis plots with no need to correct for geometric demagnetization factor. The maximum field amplitude was 144 kA/m (1.8 KOe), cycled at 0.1 to 1000 Hz. The driving fields were generated with bursts of ac current through copper wire windings. The resultant waveforms, detected with a sense winding, were electronically integrated and digitally recorded. We obtained the effective lower critical field for the intergranular coupling component as a function of temperature. [Contact: William W. Cross, (303) 497-5300]

Ekin, J.W., Hart, Jr., H.R., and Gaddipati, A.R., **Critical Current vs. Magnetic Field Characteristics of Aligned Sintered  $Y_1Ba_2Cu_3O_{7-\delta}$ .**

A study of grain alignment and its effect on the dc transport critical current  $J_c$  in bulk  $Y_1Ba_2Cu_3O_{7-\delta}$  is reported at magnetic fields from  $10^{-4}$  T to 26 T. Several unique features are found compared with polycrystalline

Superconductors (cont'd.)

$Y_1Ba_2Cu_3O_{7-\delta}$  samples. The effective upper critical field where  $J_c$  approaches zero is significantly higher for aligned samples with field parallel to the a,b planes (30 T) than it is for polycrystalline unaligned samples (7 T). Weak link effects are still found to be present at low fields (<10 mT) even though the grains in the sample were aligned, but the low-field drop in  $J_c$  is very much less than for the unaligned polycrystalline case. The plateau value of  $J_c$  for field parallel to the a,b planes is considerably enhanced to 100 to 200 A/cm<sup>2</sup> in the field range from 10 mT to 1 T. This is one to two orders of magnitude higher than typical plateau values of  $J_c$  in unaligned  $Y_1Ba_2Cu_3O_{7-\delta}$  (2 to 10 A/cm<sup>2</sup>). Data are also presented on the weak-link decoupling field, field-cooled measurements of the transport  $J_c$ , the force-free transport  $J_c$  (magnetic field oriented parallel to current), and the sharpness of the voltage-current characteristic as a function of magnetic field.

[Contact: Jack W. Ekin, (303) 497-5448]

Goldfarb, R.B., and Ishida, T., **Fundamental and Harmonic Susceptibilities of  $YBa_2Cu_3O_{7-\delta}$** .

We have examined the complex harmonic magnetic susceptibilities  $\chi_n = \chi_n' - i\chi_n''$  ( $n = 1, 2, 3, \dots, 10$ ) of the sintered high-critical-temperature superconductor  $YBa_2Cu_3O_{7-\delta}$  (YBCO). The experimental variables for the measurements of  $\chi_n$  were the sample temperature ( $10 \leq T \leq 110$  K), the ac magnetic field amplitude  $H_{ac}$  ( $1.4 \mu T \leq \mu_0 H_{ac} \leq 8.5$  mT) and frequency  $f$  ( $7.3 \leq f \leq 1460$  Hz), and the magnitude of a superimposed dc field  $H_{dc}$  ( $0 \leq \mu_0 H_{dc} \leq 8.5$  mT). As functions of temperature,  $\chi_1'$  and  $\chi_1''$  depend on both  $H_{ac}$  and  $H_{dc}$ . In particular, the  $\chi_1'$  transition curve may shift to higher temperatures with increasing  $H_{dc}$ . Odd-harmonic susceptibilities were measured as functions of temperature below  $T_c$  for zero  $H_{dc}$ ; both even and odd harmonics

were observed for nonzero  $H_{dc}$ . The temperature dependence of  $\chi_3$  is a strong function of  $H_{ac}$ .  $|\chi_3|$  has a maximum below the critical temperature  $T_c$ , similar to the peak in  $\chi_1''$ , which is slightly frequency dependent. At fixed temperature, the odd-harmonic susceptibilities are even functions of  $H_{dc}$ , while the even-harmonic susceptibilities are odd functions of  $H_{dc}$ . We compared the experimental intergrain coupling characteristics of  $\chi_n'$  and  $\chi_n''$  with theoretical susceptibility curves based on magnetization equations derived by Ji et al. from a simplified Kim model for critical current density. The theoretical curves are in good agreement with the temperature- and field-dependent features of  $\chi_n'$  and  $\chi_n''$ , and thus, the intergrain coupling component of a sintered high- $T_c$  superconductor has the properties of a type-II superconductor. [Contact: Ronald B. Goldfarb, (303) 497-3650]

Harvey, T.E., Beall, J.A., Ono, R.H., Asher, S.E., Nelson, A.J., Mason, A.R., Franz, A.B., Dhere, R., and Kazmerski, L.L., **Comprehensive Analysis of the  $YBa_2Cu_3O_7/SiTiO_3$  Interface as a Function of Post-Deposition Annealing Temperature**, to be published in the Proceedings of the Fall Meeting of the American Vacuum Society, Boston, Massachusetts, October 23-24, 1989.

X-ray diffraction and secondary ion mass spectrometry (SIMS) have been used to characterize the oriented growth and the surface and interfacial chemistry of evaporated  $YBa_2Cu_3O_7$  films grown on  $SiTiO_3$  substrates as a function of post-deposition annealing temperature. Semi-quantitative bulk compositional analysis of the films was performed by electron microprobe using x-ray wavelength dispersive spectroscopy. Diffusion of substrate species into the high-temperature superconductor films was observed at all annealing temperatures studied. In conjunction with these analyses, scanning electron microscopy (SEM) and Auger electron spectroscopy (AES) were used to determine the film

Superconductors (cont'd.)

morphology. AES analysis was also used to characterize small particles on the film surface after post-deposition annealing. X-ray diffraction data are used to compare the relative amounts of a- and c-axis growth to the morphology observed by SEM. Diffusion of substrate elements is monitored by SIMS.

[Contact: Todd E. Harvey, (303) 497-3340]

## Recently Published

Ekin, J.W., **VAMAS Interlaboratory Comparisons of Critical Current vs. Strain in Nb<sub>3</sub>Sn** [Original title: VAMAS Round Robin Results of Critical Current vs. Strain in Nb<sub>3</sub>Sn], Proceedings of the Sixth Japan/United States Workshop on High Field Superconductors, Boulder, Colorado, February 22-24, 1989, pp. 94-98.

A comparison is made of measurements of the effect of axial tensile strain on the critical current of multifilamentary Nb<sub>3</sub>Sn superconductors by three different laboratories. Two of the laboratories used short-sample testing apparatus wherein a straight section of conductor was cooled in a force-free state. One of the laboratories utilized a spring apparatus wherein a long sample was reacted in a coil shape and attached to a spring sample holder. The agreement between the results for the two laboratories utilizing the straight-sample apparatus was quite good, within 15% for all three conductors at 15 T, except at very high strain for one conductor which had an upper critical field close to the measurement field. To make a comparison with the data obtained using the spring method, it was necessary to fit the data to the compressive prestrain determined using the straight-sample technique. Making such a fit, the agreement was found to be variable, between 15 and 25% depending on the conductor. Values of the prestrain and irreversible strain obtained from the straight-sample data

agreed within 0.06% and 0.05%, respectively. Values of the maximum (strain-free) upper critical fields agreed within several tenths of a tesla.

[Contact: Jack W. Ekin, (303) 497-5448]

Ekin, J.W., Bray, S.L., Danielson, P., Smathers, D., Sabatini, R.L., and Suenaga, M., **Transverse Stress Effect on the Critical Current of Internal Tin and Bronze Process Nb<sub>3</sub>Sn Superconductors**, Proceedings of the Sixth Japan/United States Workshop on High Field Superconductors, Boulder, Colorado, February 22-24, 1989, pp. 50-52.

The effect of transverse stress on the critical current density,  $J_c$ , has been shown to be significant in bronze-process Nb<sub>3</sub>Sn, with the onset of significant degradation at about 50 MPa. In an applied field of 10 T, the magnitude of the effect is about seven times larger for transverse stress than for axial tensile stress. We have also measured the effect in an internal tin conductor with excess tin, which yields a more equiaxed Nb<sub>3</sub>Sn grain morphology than for bronze-process Nb<sub>3</sub>Sn, in which the grains tend to be more columnar. The effect of transverse stress on  $J_c$  was nearly identical for the two conductors, indicating that the transverse stress effect is probably not dependent on grain morphology.

[Contact: Jack W. Ekin, (303) 497-5448]

Ekin, J.W., Godrich, L.F., Bray, S.L., Bergren, N.F., and Goldfarb, R.B., **Electromechanical Properties of Superconductors for High-Energy Physics Applications, Part II**, NISTIR 89-3912 (November 1989).

This report presents data on superconductor performance under mechanical load. The data are needed for setting mechanical design constraints and measuring the electro-mechanical performance of NbTi superconductors for DOE high-energy physics magnet applica-

Superconductors (cont'd.)

tions. The effect of axial tensile stress, applied at room temperature, on the critical current of NbTi superconductor strands has been measured. The data show a simple result that the effect on the critical current is independent of the temperature at which the stress is applied; this allows the existing 4 K database to be used to determine critical current degradation from room temperature fabrication stress, from cool-down stress introduced by differential contraction, and from 4 K stress generated by the Lorentz force when the magnet is energized. A study of the critical-current variations along NbTi strands extracted from a Rutherford cable has been made also. The results show that the principal mechanical degradation is extremely localized at the regions where the NbTi strand is bent around the edge of the cable. For example, only 3% of the total strand length can contribute 92% of the total strand voltage. A further study has been made of the effects of bending strain on the critical current of NbTi conductors. The degradation of the critical current from bending strain is much greater at low values of electric field than at high, suggesting that irregularity of the filament cross-sectional area introduced by bending may be the source of the  $I_c$  degradation. The bend tolerance of a NbTi conductor can be enhanced by increasing the local copper-to-super conductor area ratio. Measurements of the permeability, saturation magnetization, and intrinsic coercivity of several high-permeability steel alloys were made. The overall differences of saturation magnetization and intrinsic coercivity between cold-rolled steel samples were not significant.

[Contact: Jack W. Ekin, (303) 497-5448]

Ekin, J.W., and Larson, T.M., **Magnetic-Field Angle Dependence of the Critical Current in Y-, Bi-, and Tl-Based High-TC Superconductors**, Proceedings of the

Sixth Japan/United States Workshop on High Field Superconductors, Boulder, Colorado, February 22-24, 1989, pp. 61-63.

The change in  $J_c$  with angle between applied field and current depends on the magnetic field regime. There is essentially no change at low fields, where  $J_c$  is not determined by pinning but rather by self-field effects. At intermediate fields in the plateau regime, the effect typically amounts to a 50 to 300% enhancement in  $J_c$  for the force-free case, comparable in magnitude to conventional superconductors, indicating a nearly isotropic well-connected network of percolation paths. At high fields, field angle effect becomes negligible, indicating that the percolation paths in the high-field regime become more disconnected and highly convoluted with some section of each percolation path perpendicular to the applied field independent of the angle.

[Contact: Jack W. Ekin, (303) 497-5448]

Ekin, J.W., Larson, T.M., Hermann, A.M., Sheng, Z.Z., Togano, K., and Kumakura, H., **Double-Step Critical Current vs. Field Characteristic in Y-, Bi-, and Tl-Based Bulk High- $T_c$  Superconductors**, Physica C, Vol. 160, pp. 489-496 (1989).

A double-step characteristic is observed at 76 K in the plot of transport critical current as a function of magnetic field in bulk sintered Y-, Bi-, and Tl-based high- $T_c$  superconducting materials. The low field step-like drop in the critical current commences at magnetic fields between about 0.3 and 2 mT. This is followed by a plateau region of relatively constant critical current extending from about 30 to 300 mT, and then a second drop at fields between about 0.3 and 10 T. These features occur for all three superconductor systems and are interpreted, respectively, as a weak-link regime, a remnant percolation path regime, and a

Superconductors (cont'd.)

flux flow regime.

[Contact: Jack W. Ekin, (303) 497-5448]

Goodrich, L.F., Bray, S.L., and Stauffer, T.C., **Thermal Contraction of Fiberglass-Epoxy Sample Mandrels and Its Effect on Critical-Current Measurements**, Proceedings of the Sixth Japan-U.S. Workshop on High Field Superconductors, Boulder, Colorado, February 22-24, 1989, pp. 91-93.

A systematic study of the effect of sample-mounting techniques on the superconducting critical-current measurement was made in conjunction with the VAMAS (Versailles Agreement on Advanced Materials and Standards) interlaboratory comparison measurements. A seemingly small change in mandrel geometry can result in a 40% change in the measured critical current of a Nb<sub>3</sub>Sn sample at 12 T. This is a result of a change in the conductor pre-strain at 4 K caused by variation in thermal contraction between thick- and thin-walled fiberglass-epoxy composite (G-10) tubes. An approximate measure of the variations in thermal contraction (from room to liquid nitrogen temperature) indicates a 0.2% greater contraction for the thick-walled tube. This difference, combined with strain sensitivity measurements, is consistent with the observed decrease in critical current. Previous publications on the thermal contraction of G-10 have addressed the plate geometry, but not the tube geometry. The contraction of a G-10 plate is highly anisotropic. The radial contraction of a tube is different from the contraction of a plate, however, because the circumferential fiberglass is put into hoop compression by the epoxy, and the resulting contraction is a competition between the two structural components. This appears to be the source of the variation in thermal contraction with tube wall thickness.

[Contact: Loren F. Goodrich, (303) 497-3143]

Moreland, J., Ginley, D.S., Venturini, E.L., and Morosin, B., **Break Junction Measurement of the Tunneling Gap of a Thallium-Based High-Temperature Superconductor Crystal**, Applied Physics Letters, Vol. 55, No. 14, pp. 1463-1465 (2 October 1989).

We have used the break junction method to measure the tunneling gap of a thallium-based high-temperature superconductor crystal in liquid helium at 4 K. The crystal was predominately Tl<sub>2</sub>CaBa<sub>2</sub>Cu<sub>2</sub>O<sub>7</sub> and had a superconducting onset temperature of 105 K. Tunneling data showed a symmetric gap about zero bias between two well-defined conductance peaks in the conductance versus voltage curve. The gap is consistent with a Bardeen-Cooper-Schrieffer energy gap ( $\Delta$ ) of 30 meV assuming a superconductor-insulator-superconductor electrode configuration. In addition, a supercurrent could be detected when the break junction was operated in a point-contact mode at temperatures as high as 95 K.

[Contact: John Moreland, (303) 497-3641]

Peterson, R.L., **Bean Model Extended to Magnetization Jumps**, Physics Letters A, Vol. 131, No. 2, pp. 131-134 (8 August 1988).

The Bean model of magnetization in hard superconductors is extended to include the trains of magnetization jumps seen at low temperature in moderate-to-high magnetic fields. As in the original Bean model, no particular mechanisms for flux pinning or dynamics are invoked. The model correctly accounts for the general dependence of the size of the magnetization jumps on sample size and critical current density. The data together with the model show that the shielding fields are approximately equal after each jump.

[Contact: Robert L. Peterson, (303) 497-3750/-3227]

Peterson, R.L., **Magnetization of Imperfect Superconducting Grains**,

Superconductors (cont'd.)

Physical Review B, Vol. 40, No. 4, pp. 2678-2681 (1 August 1989).

A critical-state theory of the magnetization of superconducting grains containing nonsuperconducting regions is presented which shows that the thickness of the sheath of supercurrents around these regions can be more important than the grain dimension in determining the magnetization. This may explain some apparently conflicting results on the magnetization of high- $T_c$  powders of different sizes.

[Contact: Robert L. Peterson, (303) 497-3750]

Peterson, R.L., and Ekin, J.W., **Airy Pattern, Weak-Link Modeling of Critical Currents in High- $T_c$  Superconductors**, Physica C, Vol. 157, (North-Holland, Amsterdam) pp. 325-333 (1989).

We have measured the transport critical current density at very low magnetic fields in samples of superconducting bulk sintered  $Y_1Ba_2Cu_3O_x$ ,  $Y_1Ba_2Cu_4O_x$ , and  $Ho_1Ba_2Cu_3O_x$  obtained from several sources. The results are analyzed at low fields ( $\leq 10$  mT) with a statistical model which assumes that the current is limited by Josephson weak links (SNS or SIS Josephson junctions or microbridges) whose locations are to be determined. Each weak link is assumed to be described by an Airy current-field pattern rather than a Fraunhofer pattern. The former has a better theoretical foundation and is in better agreement with the data, varying as  $H^{-3/2}$  upon averaging. The fitting procedure yields the average cross-sectional area of the weak links. By assuming the link thickness to be twice the London penetration depth at 77 K, we find that the average linear dimensions of the links are in all cases comparable to the grain dimensions. The quantitative analysis also confirms the percolation concept, in which a subset of weakest links controls the transport current.

[Contact: Robert L. Peterson, (303) 497-3750 or 3227]

Peterson, R.L., and Ekin, J.W., **Josephson-Junction Model of Critical Current in Granular  $Y_1Ba_2Cu_3O_{7-\delta}$  Superconductors**, Physical Review B, Vol. 37, No. 16, pp. 9848-9851 (1 June 1988).

We calculate the transport critical-current density in a granular superconductor in magnetic fields below about  $5 \times 10^{-3}$  T. The field dependence in this region is assumed to be controlled by intragranular or intergranular Josephson junctions. Various model calculations are fitted to transport critical-current data on bulk  $Y_1Ba_2Cu_3O_{7-\delta}$  ceramic superconductors, whose average grain size somewhat exceeds  $10 \mu\text{m}$ . The results yield an average junction cross-sectional area (thickness  $\times$  length) of 4 to  $6 \mu\text{m}^2$ . If the junctions are at the grain boundaries, a London penetration depth of about 150 to 300 nm is inferred, consistent with other estimates. We conclude that Josephson junctions are limiting the transport critical current in these samples and that they lie at the grain boundaries. The parameters of the fit are not consistent with Josephson junctions at twinning boundaries.

[Contact: Robert L. Peterson, (303) 497-3750]

Peterson, R.L., and Ekin, J.W., **Modeling of Critical Currents in Granular High- $T_c$  Superconductors**, Proceedings of Workshop on Materials Science of High  $T_c$  Superconductors, Gaithersburg, Maryland, October 11-13, 1988, pp. 190-195.

The transport critical current density of several samples of bulk sintered high- $T_c$  superconductors was measured at very low magnetic fields and fitted to a model which assumes that the impediments to current at such fields are Josephson weak links. A sample of particular interest was  $Y_1Ba_2Cu_3O_x$  made from hydroxycarbonate precursors; the final

Superconductors (cont'd.)

bulk sintered sample was very fine-grained, having an average grain size of about  $1.8 \mu\text{m}$  as determined by a linear intercept analysis. The fit to the model is excellent if the average linear dimension of the weak links is chosen to be  $2.0 \mu\text{m}$ . We conclude that this sample, as well as the others, has Josephson weak links at its grain boundaries, and that any intragrain defects which may be responsible for flux pinning are not the primary weak links limiting the transport  $J_c$  of bulk samples at very low magnetic fields. [Contact: Robert L. Peterson, (303) 497-3750]

Roshko, A., Moodera, J.S., and Chiang, Y-M., **S-N-S Behavior of Grain Boundaries in Polycrystalline  $\text{La}_{1.85}\text{Sr}_{0.15}\text{CuO}_{4-y}$** , Physica C, Vol. 162-164, pp. 1625-1626 (1989).

The field and temperature dependence of transport critical current  $J_c$  in well-characterized, polycrystalline  $\text{La}_{1.85}\text{Sr}_{0.15}\text{CuO}_{4-y}$  has been investigated. The behavior at low fields, close to critical temperature  $T_c$ , corresponds to that of superconductor-normal-superconductor (S-N-S) junctions. [Contact: Alexana Roshko, (303) 497-5420]

Magnetic Materials & Measurements

Released for Publication

Cross, R.W., and Goldfarb, R.B., **Variable Frequency Magnetometer for Superconductor Toroids.**

We constructed a flux-integration magnetometer and made magnetization measurements on a toroidal sample of  $\text{YBa}_2\text{Cu}_3\text{O}_x$  high-critical-temperature superconductor as a function of magnetic field amplitude, frequency, and temperature. The toroid geometry gives calibrated hysteresis plots with no need to correct for geometric demagnetization factor. The maximum field amplitude was

144 kA/m (1.8 KOe), cycled at 0.1 to 1000 Hz. The driving fields were generated with bursts of ac current through copper wire windings. The resultant waveforms, detected with a sense winding, were electronically integrated and digitally recorded. We obtained the effective lower critical field for the intergranular coupling component as a function of temperature. [Contact: William W. Cross, (303) 497-5300]

Cross, R.W., Patton, C.E., Srinivasan, G., Booth, J.G., and Chen, M., **Anomalous Low Frequency Butterfly Curves for Subsidiary Absorption and FMR Overlap at 3 GHz.**

Subsidiary absorption butterfly curves of spin-wave instability threshold versus static in-plane magnetic field have been obtained for yttrium-iron-garnet (YIG) thin films at 3 GHz. The butterfly curves have been found to be rather anomalous, typically displaying a pronounced dip and a very low minimum threshold. These anomalous features are attributed to the overlap of the subsidiary absorption field region with ferromagnetic resonance (FMR). First-order instability theory was extended to include the uniform mode response near FMR. The extended theory yields good fits to the data for reasonable values of the YIG FMR linewidths. The analysis also yields a new prediction of a flip in the azimuthal propagation angle  $\phi_k$  for the unstable spin waves in the region of FMR overlap. With increasing field, there are predicted discontinuous changes in  $\phi_k$  from  $90^\circ$  to  $0^\circ$  and back to  $90^\circ$  in the region of FMR.

[Contact: William R. Cross, (303) 497-5300]

ELECTROMAGNETIC INTERFERENCERadiated Electromagnetic Interference

Released for Publication

Hill, D.A., **Quasi-Static Analysis of a Two-Wire Transmission Line Located at**

Radiated EMI (cont'd.)

## an Interface.

Simple quasi-static expressions have been derived for the propagation constant, the characteristic impedance, and the field distribution of a two-wire transmission line located at the air-earth interface. Both the complex permittivity and the complex permeability of the earth are allowed to differ from the free-space values, and a numerical solution of the mode equation shows that quasi-static approximation is valid when the wire separation is much less than a free-space wavelength. The quasi-static approximation can be used to determine both the complex permittivity and the complex permeability of the earth from measurements of the propagation constant and the characteristic impedance of the transmission line.

[Contact: David A. Hill, (303) 497-3472]

Wilson, P.F., and Ma, M.T., **Fields Radiated by Electrostatic Discharges.**

Electrostatic discharge (ESD) metrology has, to date, primarily focused on the ESD current waveforms in order to develop simulators for susceptibility testing. Significantly less attention has been given to the fields generated by an ESD event. This paper examines ESD fields both analytically and experimentally. Measurements indicate that the electric fields can be quite significant ( $\geq 150$  V/m at a distance of 1.5 m, for example) for short periods of time (a few nanoseconds), particularly for relatively low voltage events ( $\leq 6$  kV). A relatively simple dipole model of an ESD spark is developed and used to predict the radiated fields. The agreement between theory and experiment is reasonable. The model may be used to predict ESD fields for a wide range of possible configurations, particularly in the near-field zone where no measurements are presently

available.

[Contact: Mark T. Ma, (303) 497-3800]

Wittmann, R.C., **Spherical Near-Field Scanning: Determining the Incident Field Near a Rotatable Probe**, to be published in the Proceedings of the International Symposium on Antennas and Propagation, Dallas, Texas, May 7-11, 1990.

Many radar cross-section, electromagnetic interference/electromagnetic compatibility, and antenna measurements require a known incident field within a test volume. To evaluate systems designed to produce a specific incident field (compact ranges, for example), we must measure the actual illumination for comparison with design specifications. Beyond its diagnostic value, these incident field data can also be used for error estimation and for calculating first-order corrections.

In this paper, we develop a spherical near-field scanning algorithm for determining incident fields inside a probe's "minimum sphere." This differs from the well-known spherical near-field scanning formulation which determines fields outside the source's minimum sphere. The scanner size depends on the extent of the region of interest and not on the extent of the (possibly much larger) source. The data may be collected using a standard roll-over-azimuth positioner.

[Contact: Ronald C. Wittmann, (303) 497-2236]

## Recently Published

Adams, J.W., Ondrejka, A.R., Cavcey, K.H., Cruz, J.E., Medley, H.W., and Grosvenor, Jr., J.H., **Recent Improvements in Time-Domain EMC Measurement System**, NISTIR 89-3927 (November 1989).

Improved techniques for determining critical resonant frequencies and the current response of internal wiring due to external fields for rotary-wing aircraft are given. The measurement

Radiated EMI (cont'd.)

method uses a train of low-level, radiated pulses. These do not disturb other spectrum users, nor do other spectrum users significantly disturb these measurements. The fields are low, a distinct advantage from both cost and personnel hazard standpoints. The problems that should be addressed before the full potential of the technique can be realized are discussed.

[Contact: John W. Adams, (303) 497-3328]

Hill, D.A., and Ehret, R.L., **Near-Field Gain of Pyramidal Horns from 18 to 40 GHz**, NISTIR 89-3924 (November 1989).

Generating a standard electromagnetic field requires knowledge of the gain of the transmitting antenna. Using the two-antenna method, we have measured the near-field gain of pyramidal horns at frequencies from 18 to 40 GHz. The discrepancy between the measured and theoretical near-field gain is typically within  $\pm 0.3$  dB for distances from 0.5 to 4 m from the horn aperture. An accurate laser alignment of the horns was necessary to obtain this level of agreement.

[Contact: David A. Hill, (303) 497-3472]

Ma, M.T., and Crawford, M.L., **Facilities for Improving Evaluations of Electromagnetic Susceptibilities of Weapon Systems and Electronic Equipment**, NISTIR 89-3928 (November 1989).

A preliminary design of an improved testing facility for evaluating the electromagnetic susceptibility of weapon systems and electronic equipment is presented. This facility features a combination of the transverse electromagnetic (TEM) cell for low-frequency testing and the reverberating chamber for high-frequency operation. As a system, a coverage of the wide spectrum from 10 kHz to 18 GHz or even to 40 GHz is possible. The TEM/reverberating

combination is designed for an input impedance to 50, 75, or 100  $\Omega$  to generate a continuous-wave electric field up to 200 V/m, or a pulsed electric field up to 50 kV/m with an approximate rise time of 10 ns. The average field for the reverberating mode of operation is described in a statistical sense. Theoretical characteristics for a case study, to meet a given set of requirements, are given.

[Contact: Mark T. Ma, (303) 497-3800]

Randa, J.P., and Kanda, M., **Standard Field Generation for Microwaves and Millimeter Waves**, Navy Metrology, Research & Development Requirements Conference Report, Corona, California, April 4-6, 1989, pp. 97-100 (April 1989).

The requirements for electromagnetic field measurements at microwave and millimeter-wave frequencies in both the laboratory and the field are discussed. Current National Institute of Standards and Technology (NIST) capabilities and intended extensions are presented. The NIST anechoic-chamber facility can generate calibrated fields up to 18 GHz and will soon be extended to 40 GHz. Future extensions will be 2-GHz bands centered at 60 GHz and 95 GHz. Transfer-standard probes developed by NIST are available up to 18 GHz, and work is in progress to develop probes which would operate to 110 GHz. It is not clear whether these probes (if successfully developed) would be suitable for field use, as hazard meters, for example. For measurements in the field, electric-field probes which are claimed to operate to 40 GHz are available commercially. Small, transportable facilities for calibration of probes in the field are not readily available. This paper discusses the present situation in these areas, presents current NIST work to extend our relevant capabilities, and notes present and probable future deficiencies.

[Contact: James P. Randa, (303) 497-3150]

**ADDITIONAL INFORMATION**Lists of Publications

Lyons, R.M., and Gibson, K.A., **A Bibliography of the NIST Electromagnetic Fields Division Publications**, NISTIR 89-3920 (September 1989).

This bibliography lists publications by the staff of the National Institute of Standards and Technology's Electromagnetic Fields Division for the period from January 1970 through August 1989. Selected earlier publications from the Division's predecessor organizations are included.

[Contact: Kathryn A. Gibson, (303) 497-3132]

DeWeese, M.E., **Metrology for Electromagnetic Technology: A Bibliography of NIST Publications**, NISTIR 89-3921 (August 1989).

This bibliography lists the publications of the personnel of the Electromagnetic Technology Division of NIST in the period from January 1970 through publication of this report. A few earlier references that are directly related to the present work of the Division are included.

[Contact: Sarabeth Moynihan, (303) 497-3678]

Palla, J.C., and Meiselman, B., **Electrical and Electronic Metrology: A Bibliography of NIST Electricity Division's Publications**, NIST List of Publications 94 (January 1990).

This bibliography covers publications of the Electricity Division, Center for Electronics and Electrical Engineering, NIST, and of its predecessor sections for the period January 1968 to December 1989. A brief description of the Division's technical program is given in the introduction.

[Contact: Jenny C. Palla, (301) 975-2220]

Walters, E.J., **Semiconductor Measurement**

**Technology, NBS List of Publications 72** [a bibliography of NBS publications concerning semiconductor measurement technology for the years 1962-1989] (March 1990).

This bibliography contains reports of work performed at the National Institute of Standards and Technology in the field of Semiconductor Measurement Technology in the period from 1962 through December 1989. An index by topic area and a list of authors are provided.

[Contact: E. Jane Walters, (301) 975-2050]

**NEW CALIBRATION SERVICES OFFERED**

The explosive growth of optical fiber use in the communications industry has resulted in a demand for calibration services. NIST's Boulder, Colorado, laboratory now offers **measurements of optical laser power and energy at wavelengths and power levels of interest to fiber optic producers and users.** Measurements are based on a standard reference instrument called the C-series calorimeter. An electrically calibrated pyroelectric radiometer (ECPR) is calibrated against the calorimeter and is then used to calibrate optical power meters at wavelengths of 850, 1300, and 1550 nm. To improve calibration capabilities, NIST is preparing test measurement systems for detector linearity, detector uniformity, and detector spectral responsivity. These systems should be available in 6 months. For a paper outlining NIST's optical power measurement capabilities, contact Fred McGehan, Div. 360, NIST, 325 Broadway, Boulder, Colorado 80303. For more information on calibration services, contact Thomas R. Scott, Div. 724, same address, or phone (303) 497-3651.

**NEW NIST RESEARCH MATERIAL**

NIST has announced the availability of **Research Material 8458**, a well-characterized artificial flaw used as an artifact standard in eddy current

New NIST Research Material (cont'd.)

**nondestructive evaluation (NDE).** The new Research Material (RM) is the outcome of work carried out by the Division to address the need for calibration standards for eddy-current NDE, for example as used to detect fatigue cracks in aircraft structures. The RM flaw is produced in an annealed aluminum alloy block by first indenting the block and then compressively deforming the resulting notch until it is tightly closed. The next operation is to restore a flat finish to the block face, after which the block is heat treated to the original temper. The controlled flaw has been named the "CDF notch," after its inventors (listed on patent application) Thomas E. Capobianco (Electromagnetic Technology Division), William P. Dube (Division 583), and Ken Fizer (Naval Aviation Depot, NAS Norfolk, Virginia).

In the past, the challenge has been to manufacture artificial flaws that closely simulate the mechanical properties of fatigue cracks. Currently used artifacts include electrical-discharge-machined and saw-cut notches, both of which are relatively poor representations of fatigue cracks as their widths are too great. The Division-developed method provides notches that can be made controllably in a variety of geometries, have known dimensions, with widths that are narrow enough to provide an acceptable representation of fatigue cracks.

An NIST Research Material is not certified by NIST, but meets the International Standards Organization definition of "a material or substance one or more properties of which are sufficiently well established to be used in the calibration of an apparatus, the assessment of a measurement method, or for assigning values to materials." The documentation issued with RM 8458 is a "Report of Investigation." Contact: technical information -- Fred Fickett, (303) 497-3785; order information--

Office of Standard Reference Materials,  
(301) 975-6776.

**JAN. 1, 1990 CHANGES IN THE U.S.  
ELECTRICAL UNITS**

Effective January 1, 1990, the U.S. as-maintained (i.e., "practical") units of voltage and resistance were increased by 9.264 ppm and 1.69 ppm, respectively. The increases in the U.S. legal units of current and of electrical power will be about 7.57 ppm and 16.84 ppm, respectively. These changes result from efforts by the major national standardizing laboratories, including the National Institute of Standards and Technology (NIST), formerly the National Bureau of Standards (NBS), to re-evaluate their as-maintained units in terms of the International System of Units (SI). The consequence of this activity has been the introduction of standards representing the SI units of voltage and resistance by the International Committee of Weights and Measures, an international body created by the Treaty of the Meter.<sup>1</sup> The use of these standards world-wide beginning January 1, 1990, will result in international consistency of electrical measurement as well as coherence among the practical units of length, mass, electricity, time, etc., inherent in the definitions of the SI.

Implementation of Changes at NIST

These changes have been instituted in the U.S. by NIST using the new, internationally-adopted constants  $K_{J-90} = 483\,597.9$  GHz/V exactly and  $R_{K-90} = 25\,812.807$   $\Omega$  exactly with the Josephson and quantum Hall effects to establish representations of the SI volt and ohm,

<sup>1</sup>Note that the SI Units have not been redefined; rather, they have been realized more accurately and a quantum physics representation of the ohm has been introduced, thus leading to the changes in magnitude of the practical or as-maintained units.

Changes in U.S. Elec. Units (cont'd.)

respectively. The representation of the SI volt is attained by using  $K_J$  in the formula

$$U_J(n) = \frac{f}{K_J} \quad n = 1, 2, 3, \dots$$

to give the voltages  $U_J(n)$  of the steps produced by the ac Josephson effect at a frequency  $f$ . The past value,  $K_{J-72}$ , was 483 593.42 GHz/V(NBS-72), thus leading to the 9.264 ppm change. Likewise,  $R_K$  is used in the following formula for the resistance of the  $i^{th}$  plateau of a quantum Hall effect device,

$$R_H(i) = \frac{R_K}{i} \quad (R_K = R_H(1))$$

to realize a representation of the SI ohm. The most recent past national unit of resistance,  $\Omega(NBS-48)_t$ , was based on a group of five Thomas one-ohm standards and had an uncompensated drift rate of approximately -0.053 ppm per year. Since the quantum Hall effect is used as the national standard, the U.S. representation of the ohm has no drift. (The past unit of voltage, V(NBS-72), was based on the Josephson effect since 1972, and accordingly had a zero drift rate.)

Reassignments to Non-adjustable Standards

Since the U.S. practical volt and ohm units increased on January 1, 1990, the changes must be implemented in non-adjustable standards calibrated in terms of V(NBS-72) and/or  $\Omega(NBS-48)$  only by reducing the values assigned to them proportionally. The examples given below show how to do this for a standard cell and a standard resistor.

Sample Adjustments of Values of Standards

Standard cell:

"Old" emf 1.0180564 V(NBS-72)

Multiply "Old" emf by 0.999990736 to get emf in terms of the present volt representation  $1.01804697 \approx 1.0180470$  V

Standard resistor:

"Old" resistance value  
 $9999.976 \Omega(NBS-48)_{01/01/90}$

Multiply "Old" resistance by 0.99999831 to get the resistance in terms of the present ohm representation  
 $9999.9591 \approx 9999.959 \Omega$

In the above, "Old" refers to the value of the standard which would have been in use on January 1, 1990, had the changes not been made; i.e., if a correction curve based on its past assigned values has been employed to obtain the currently-used value for a standard, the above represents a downward shift of the curve starting January 1, 1990. For resistance, the slope of the curve also changed (slightly) since  $\Omega(NBS-48)$  has a drift rate and  $\Omega(NIST-90)$  does not.

Do not send your standards to NIST for recalibration on January 1, 1990, unless they are normally due then. The changes are accurately known and corrections to existing standards may be applied.

Adjustment of Instrumentation

An assigned or calibrated value of a standard is merely a label giving the magnitude of the parameter embodied in the standard. The actual emf or resistance of a standard did not change on January 1, 1990; only what it is called should have changed. In the same sense, meter readings are labels giving the magnitudes of the parameters being measured. Readings taken after January 1, 1990 using unadjusted meters will be too large in magnitude. Adjustments to meters must have the effect of reducing the amplitudes of readings for fixed emf's or resistances.

Adjustable voltage and current sources

Changes in U.S. Elec. Units (cont'd.)

or adjustable resistors for which nominal output is desired, on the other hand, must have their outputs **increased** proportionally by the above amounts. DVM calibrators are probably the largest class of this type of instrument.

Guidelines

The National Conference of Standards Laboratories (NCSL) and NIST have formed NCSL ad hoc Committee 91.4, Changes in the Volt and Ohm to assist industry and government laboratories in coming into compliance with the changes. A major responsibility of the committee is the generation and publication of a set of guidelines which describes unambiguous methods for adjusting standards and instruments, or their values, and delineates other types of problems which may arise, e.g., voltage values called out explicitly in maintenance procedures, values imbedded in software, and the like. These guidelines have been published as NIST Technical Note 1263, "Guidelines for Implementing the New Representations of the Volt and Ohm Effective January 1, 1990." This document is available at no charge through the NIST Electricity Division. To receive a copy, contact Sharon Fromm at 301-975-4222.

For further information, contact Norman B. Belecki (301-975-4223), Ronald F. Dziuba (301-975-4239), Bruce F. Field (301-975-4230), or Barry N. Taylor (301-975-4220).

**U.S. REPRESENTATIONS OF ELECTRICAL POWER AND ENERGY**

Watt, Var, Volt-Ampere  
Joule, Watthour, Varhour  
Volt-Ampere-hour, and Q-hour

Background

By international agreement, starting on

January 1, 1990, the U.S. put into place new representations of the volt and ohm based, respectively, on the Josephson and Quantum Hall effects and which are consistent with the International Systems of Units (SI). Implementation of the new volt and ohm representations in the U.S. required that on January 1, 1990, the value of the present national volt representation maintained by the National Institute of Standards and Technology (NIST, formerly the National Bureau of Standards) be increased by 9.264 parts per million (ppm) and that the value of the national ohm representation be increased by 1.69 ppm (1 ppm = 0.0001%). The resulting increase in the national representation of the ampere is 7.57 ppm. The resulting increase in the national representations of the electrical quantities of power, namely the watt, var, and volt-ampere, and the quantities of energy, namely the joule, watthour, varhour, volt-ampere-hour, and Q-hour is 16.84 ppm.

The adjustment for electrical power and energy is generally very small compared to revenue metering measurement uncertainties (typically greater than  $\pm 0.1\%$ ) and therefore are not likely to have a significant effect. Adjustments do not need to be applied in these instances. However, for the highest accuracy calibrations of power and energy standards having uncertainties less than  $\pm 0.020\%$  ( $\pm 200$  ppm), adjustments should be made. Accordingly, all Reports of Calibration and Reports of Test issued by NIST after January 1, 1990, reflect the appropriate changes.

For instruments calibrated prior to January 1, 1990, adjustments to the calibration values due to the change in the volt and ohm can be made without instrument recalibration. The adjustments are exact and, if properly applied, will not introduce any errors. Examples given below illustrate proper procedures for applying the new adjustments.

Electrical Power & Energy (cont'd.)

$$(120 \text{ V} \times 5 \text{ A} \times 1)] \times 100 = \pm 0.010\%$$

Adjustments for Wattmeters, Varmeters, and Volt-Ampere Meters

Calibrations of wattmeters, varmeters, and volt-ampere meters at NIST provide customers with corrections and uncertainties given in units of watts, vars, or volt-amperes, as appropriate. Applying the appropriate adjustment due to the new representations of the volt and ohm for power measuring instruments (i.e., wattmeters for "real power" and varmeters for quadrature or imaginary power) requires minor calculations. First, it is necessary to assess the magnitude of the calibration uncertainty in percent and then decide if applying the adjustments for the change in the volt and ohm are required. To determine the percentage uncertainty, divide the uncertainty in watts, vars, or volt-amperes by the product of the applied voltage and current times the power factor (the real power) and multiply that quantity by 100, as

$$U\% = [(U_w, U_v, \text{ or } U_{va}) / (V_a \times I_a \times PF)] \times 100,$$

where

- U% is the uncertainty in percent,
- U<sub>w</sub> is the calibration uncertainty in watts,
- U<sub>v</sub> is the calibration uncertainty in vars,
- U<sub>va</sub> is the calibration uncertainty in volt-amperes,
- V<sub>a</sub> is the applied voltage in volts,
- I<sub>a</sub> is the applied current in amperes, and
- PF is the power factor (including its sign).

For example, if the uncertainty is stated on a Report of Calibration as ±0.060 watts for the calibration of a wattmeter at an applied voltage of 120 V and an applied current of 5 A at unity power factor, then

$$\text{Percent Uncertainty} = U\% = [(\pm 0.060 \text{ W}) /$$

If the percentage uncertainty, as calculated above, is less than ±0.020%, (as it is in the above example), then it is recommended that an adjustment due to the new representations of the volt and ohm of 0.0017% (0.001684% rounded to four significant decimal places) be applied.

The second step is the calculation of how large the adjustment will be (in units of watts, vars, or volt-amperes, as appropriate), due to the reassignment of the volt and ohm. For the same example given above, if the calibration correction was given in a Report of Calibration as +0.052 watts, then the adjustment due to the change in the volt and ohm may be calculated by multiplying the product of the applied voltage and current times the power factor by 0.000017 (0.0017% expressed in proportional parts), as

$$\begin{aligned} \text{Adjustment} &= (V_a \times I_a \times PF) \times 0.000017 \\ \text{Adjustment} &= (120 \text{ V} \times 5 \text{ A} \times 1) \times 0.000017 = 0.010 \text{ watts.} \end{aligned}$$

The resulting product should be rounded to the same number of significant decimal places as the old calibration correction was given. This result is then subtracted from the old calibration correction, as in the following example:

Old Calibration Correction	
(prior to 1/1/90) =	{+0.052 watts}
less 0.000017 x Applied	
Volt-amperes x PF =	<u>-(+0.010 watts)</u>
New Calibration Correction	
(after 1/1/90) =	{+0.042 watts}

If the old calibration correction (prior to 1/1/90) at test conditions of 120 V, 5 A, and at a power factor of 0.5 lag, happened to be a negative quantity, for example, -0.031 watts, then the old calibrations correction would be decreased (made more negative) by 0.0017% of the applied volt-ampere product times the power factor, as in

Electrical Power & Energy (cont'd.)

the following example:

Old Calibration Correction  
 (prior to 1/1/90) = {-0.031 watts}  
 less 0.000017 x Applied  
 Volt-amperes x PF = -(+0.005 watts)  
 New Calibration Correction  
 (after 1/1/90) = {-0.036 watts}

The process of making the corresponding change for the varmeter corrections is identical to that shown above. For volt-ampere meters, the adjustment is made independent of the power factor (i.e., a value of PF = 1 may be used). However, most varmeter and volt-ampere meter calibrations have stated uncertainties greater than  $\pm 0.020\%$ , and hence would not require an adjustment.

Adjustments for Joule, Watt-, Var-, Volt-Ampere- and Q-Hour Meters

Applying adjustments to electric energy measuring instruments (i.e., joule, watthour, varhour, volt-ampere-hour, and Q-hour meters) for changes in the representation of the volt and ohm, is more straightforward because the common calibration constant for energy metering is expressed as a "percentage registration." The amount the registration is to be adjusted can be subtracted directly as a percentage, regardless of power factor.

For example, if a watthour meter has a registration of 100.015% before January 1, 1990, then after that date, the new assigned registration would be decreased by 0.0017% (rounded from 0.001684%) as

Old percentage registration  
 (prior to 1/1/90) = 100.015%  
 less amount due to change  
 in volt and ohm = -0.0017%  
 New percentage registration  
 (after 1/1/90) = 100.0133%  
 Rounded to three significant  
 decimal places = 100.013%

The process of making the corresponding

changes for the joule, varhour, volt-ampere-hour and Q-hour meters are identical to that shown above. If the associated uncertainty of the calibration is greater than  $\pm 0.020\%$ , no adjustments are necessary, as stated in the instances for wattmeters, varmeters, and volt-ampere meters. The uncertainties for varhour, volt-ampere-hour, and Q-hour meters are seldom less than  $\pm 0.020\%$ , and hence adjustments generally do not need to be made.

Reference

N.B. Belecki, R.F. Dziuba, B.F. Field, and B.N. Taylor, **Guidelines for Implementing the New Representations of the Volt and Ohm Effective January 1, 1990**, NIST Technical Note 1263, June, 1989.

Copies of the above document are available at no cost from:

National Institute of Standards and Technology  
 Electricity Division, MET B146  
 Gaithersburg, MD 20899  
 Telephone: (301) 975-4222

For Further Information

For further information concerning the above information, contact either John D. Ramboz (301) 975-2434 or Thomas L. Nelson (310) 975-2427, or write:

National Institute of Standards and Technology  
 Electricity Division, MET B344  
 Gaithersburg, MD 20899

NEW BROCHURE FOR SEMICONDUCTOR SRMs

Standard Reference Materials for Semiconductor Manufacturing Technology lists a series of SRMs for use in characterizing semiconductor materials and processes. The SRMs include a series of silicon resistivity materials for calibrating four-probe and eddy-current test equipment, sizing materials for calibrating optical and scanning

New Brochure (cont'd.)

electron microscopes, SRMs for mechanical testing, optical measurements, X-ray and photographic films, X-ray diffraction, and the chemical analysis of materials.

[Contact: Roger Rensberger, (301) 975-2762]

**1990 CEEE CALENDAR**

August 28-31 (Vail and Boulder, CO)

**Laser Measurements Short Course.** In cooperation with the University of Colorado and industry, NIST is offering a three-and-one-half day course emphasizing the concepts, techniques, and apparatus used in measuring laser parameters. Topics in the course syllabus include optics for laser measurements, attenuation techniques, laser operation, basic laser power/energy standards, laser power/energy measurement techniques, optical fiber power measurements, pulse measurements, transfer standards, beam-profile measurements, diode lasers, laser measurements for optical communications, statistics and error analysis, laser safety, and detectors. The course will incorporate a visit to the NIST laser measurement laboratories. [Contact: Thomas Scott, (303) 497-3651 or Office of Conference Services, University of Colorado at Boulder, (303) 492-5151]

September 11-12, 1990 (Boulder, CO)

**Symposium on Optical Fiber Measurements.** NIST, in cooperation with the Institute of Electrical and Electronics Engineers Optical Communications Committee and the Optical Society of America, will sponsor the 6th Biennial Symposium on Optical Fiber Measurements. The symposium will be devoted entirely to measurements on fiber, related components, and systems. Typical topics will include telecommunications fibers, fiber lasers and amplifiers, fibers for sensors, couplers, connectors, multiplexers, integrated optics, sources, detectors,

modulators, switches, long haul systems, LANs, subscriber loops, field and laboratory instrumentation, and standards. Experimental and analytical papers are solicited on any aspect of measurements for guided-lightwave technology.

[Contact: Douglas L. Franzen, (303) 497-3346.]

September 17-19, 1990 (Boston, MA)

**VLSI and GaAs Chip Packaging Workshop.** The IEEE CHMT Society and the National Institute of Standards and Technology are co-sponsoring the Ninth VLSI packaging Workshop. Topics to be discussed include VLSI package design; multichip module design; WSI packaging; package thermal design; package electrical design; GaAs IC packaging; VLSI package interconnection options; VLSI package materials and die-attach solutions; and failure mechanism and quality of VLSI packages. All attendees are expected to be specialists working in the field and to participate in discussions.

[Contact: George G. Harman, (301) 975-2097]

October 24-26 (Boulder, CO)

**Symposium on Optical Materials for High Power Lasers** (Boulder Damage Symposium). The Symposium is the principal forum for the exchange of information on the physics and technology of materials for high-power lasers. Co-sponsors in addition to NIST are ASTM -- Standards for Materials, Products, Systems & Services; the Center for Research in Electro-Optics and Lasers at the University of Central Florida; the Defense Advanced Research Projects Agency; Lawrence Livermore National Laboratory, Los Alamos National Laboratory; SPIE -- the International Society for Optical Engineering; and the Weapons Laboratory of the U.S. Air Force. Topics on the agenda include new materials, bulk damage phenomena, surface and thin-film damage, preparation of optical material, measurement of

1990 CEEE Calendar (cont'd.)

optical material properties, design consideration for high-power systems, and fundamental mechanisms of laser-induced damage. [Contact: Aaron A. Sanders, (303) 497-5341]

**CEEE SPONSORS**

National Institute of Standards and Technology

U.S. Air Force

Hanscom Field; Rome Air Development Center; Space & Missile Organization; U.S. Air Force Headquarters; Wright-Patterson Air Force Base

U.S. Army

Fort Belvoir; Fort Monmouth; Fort Huachuca; Materials & Mechanics Research Center; Strategic Defense Command; Dugway Proving Ground; Strategic Defense Initiative Organization; AVRADCOM (Aviation)

Department of Defense

Advanced Research Projects Agency; Defense Communication Agency; Defense

Nuclear Agency; Combined Army/Navy/Air Force (CCG)

Department of Energy

Energy Systems Research; Fusion Energy; Basic Energy Sciences; High Energy & Nuclear Physics

Department of Justice

Law Enforcement Assistance Administration

U.S. Navy

Naval Ocean Systems Center; Naval Sea Systems Command; Weapons Support Center/Crane; Office of Naval Research; Naval Ship Research Development Center; Naval Air Systems Command; Aviation Logistics Center/Patuxent

National Science Foundation

National Aeronautics and Space Administration

Goddard Space Flight Center; Lewis Research Center

Nuclear Regulatory Commission

Department of Transportation

National Highway Traffic Safety Administration

MIMIC Consortium

Various Federal Government Agencies

1. PUBLICATION OR REPORT NUMBER NISTIR 4323
2. PERFORMING ORGANIZATION REPORT NUMBER
3. PUBLICATION DATE June 1990

# BIBLIOGRAPHIC DATA SHEET

**TITLE AND SUBTITLE**  
Center for Electronics and Electrical Engineering Technical Progress Bulletin Covering  
Center Programs, October to December 1989, with 1990 CEEE Events Calendar

**AUTHOR(S)**  
A. Gonzalez, compiler

**PERFORMING ORGANIZATION (IF JOINT OR OTHER THAN NIST, SEE INSTRUCTIONS)**  
U.S. DEPARTMENT OF COMMERCE  
NATIONAL INSTITUTE OF STANDARDS AND TECHNOLOGY  
GAITHERSBURG, MD 20899

7. CONTRACT/GRANT NUMBER  
  
8. TYPE OF REPORT AND PERIOD COVERED  
October-December 1989

**SPONSORING ORGANIZATION NAME AND COMPLETE ADDRESS (STREET, CITY, STATE, ZIP)**

**SUPPLEMENTARY NOTES**  
All technical information included in this document has been approved for publication  
previously.  
 DOCUMENT DESCRIBES A COMPUTER PROGRAM; SF-185, FIPS SOFTWARE SUMMARY, IS ATTACHED.

**ABSTRACT (A 200-WORD OR LESS FACTUAL SUMMARY OF MOST SIGNIFICANT INFORMATION. IF DOCUMENT INCLUDES A SIGNIFICANT BIBLIOGRAPHY OR LITERATURE SURVEY, MENTION IT HERE.)**

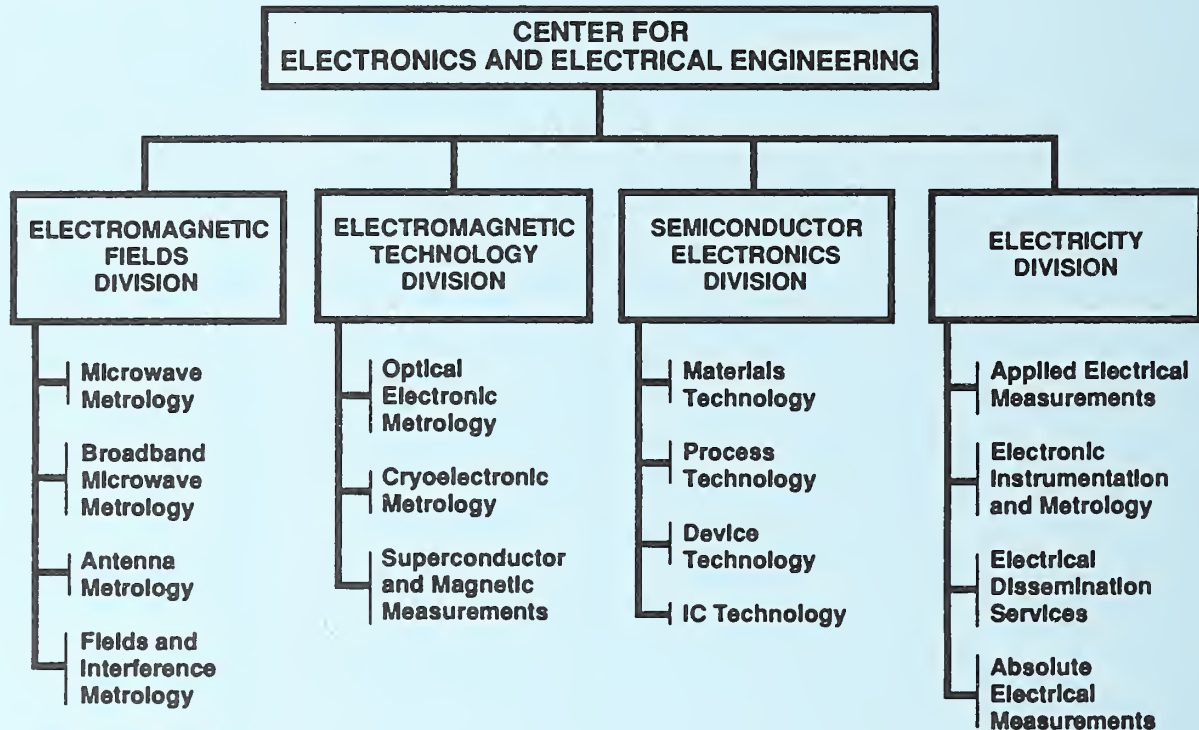
This is the twenty-ninth issue of a quarterly publication providing information on  
the technical work of the National Institute of Standards and Technology (formerly the  
National Bureau of Standards) Center for Electronics and Electrical Engineering. This  
issue of the CEEE Technical Progress Bulletin covers the fourth quarter of calendar  
year 1989. Abstracts are provided by technical area for both published papers and  
papers approved by NIST for publication.

**KEY WORDS (6 TO 12 ENTRIES; ALPHABETICAL ORDER; CAPITALIZE ONLY PROPER NAMES; AND SEPARATE KEY WORDS BY SEMICOLONS)**  
antennas; electrical engineering; electrical power; electromagnetic interference;  
electronics; instrumentation; laser; magnetics; microwave; optical fibers;  
semiconductors; superconductors

**AVAILABILITY**  
 UNLIMITED  
FOR OFFICIAL DISTRIBUTION. DO NOT RELEASE TO NATIONAL TECHNICAL INFORMATION SERVICE (NTIS).  
ORDER FROM SUPERINTENDENT OF DOCUMENTS, U.S. GOVERNMENT PRINTING OFFICE,  
WASHINGTON, DC 20402.  
 ORDER FROM NATIONAL TECHNICAL INFORMATION SERVICE (NTIS), SPRINGFIELD, VA 22161.

14. NUMBER OF PRINTED PAGES  
46  
15. PRICE  
A03

OFFICIAL BUSINESS  
PENALTY FOR PRIVATE USE, \$300



NIST / CEEE / MAY 90

**KEY CONTACTS**

Center Headquarters (720)

Electromagnetic Fields Division (723)

Electromagnetic Technology Division (724)

Semiconductor Electronics Division (727)

Electricity Division (728)

Director, Mr. Judson C. French (301) 975-2220

Deputy Director, Mr. Robert I. Scace (301) 975-2220

Chief, Dr. Ramon C. Baird (303) 497-3131

Chief, Dr. Robert A. Kamper (303) 497-3535

Chief, Mr. Frank F. Oettinger (301) 975-2054

Chief, Dr. Oskars Petersons (301) 975-2400

**INFORMATION:**

For additional information on the Center for Electronics and Electrical Engineering, write or call:

Center for Electronics and Electrical Engineering  
National Institute of Standards and Technology  
Metrology Building, Room B-358  
Gaithersburg, MD 20899  
Telephone (301) 975-2220